Deep Neural Networks for Estimation and Inference: Application to Causal Effects and Other Semiparametric Estimands*

Max H. Farrell   Tengyuan Liang   Sanjog Misra

University of Chicago, Booth School of Business

December 14, 2018

Abstract

We study deep neural networks and their use in semiparametric inference. We prove valid inference after first-step estimation with deep learning, a result new to the literature. We provide new rates of convergence for deep feedforward neural nets and, because our rates are sufficiently fast (in some cases minimax optimal), obtain valid semiparametric inference. Our estimation rates and semiparametric inference results handle the current standard architecture: fully connected feedforward neural networks (multi-layer perceptrons), with the now-common rectified linear unit activation function and a depth explicitly diverging with the sample size. We discuss other architectures as well, including fixed-width, very deep networks. We establish nonasymptotic bounds for these deep nets for nonparametric regression, covering the standard least squares and logistic losses in particular. We then apply our theory to develop semiparametric inference, focusing on treatment effects, expected welfare, and decomposition effects for concreteness. Inference in many other semiparametric contexts can be readily obtained. We demonstrate the effectiveness of deep learning with a Monte Carlo analysis and an empirical application to direct mail marketing.

Keywords: Deep Learning, Rectified Linear Unit, Nonasymptotic Bounds, Semiparametric Inference, Treatment Effects, Program Evaluation, Treatment Targeting.

1 Introduction

Statistical machine learning methods are being rapidly integrated into the social and medical sciences. Economics is no exception, and there has been a recent surge of research that applies and explores machine learning methods in the context of econometric modeling, particularly in "big data" settings. Furthermore, theoretical properties of these methods are the subject of intense recent study. This has netted several breakthroughs both theoretically, such as robust, valid inference following machine learning, and in novel applications and conclusions. Our goal in the

present work is to study a particular statistical machine learning technique which is widely popular in industrial applications, but infrequently used in academic work and largely ignored in recent theoretical developments on inference: deep neural networks. To our knowledge we provide the first inference results using deep learning methods.

Neural networks are estimation methods that model the relationship between inputs and outputs using layers of connected computational units (neurons), patterned after the biological neural networks of brains. These computational units sit between the inputs and output and allow data-driven learning of the appropriate model, in addition to learning the parameters of that model. Put into more familiar nonparametric terms: neural networks can be thought of as a (complex) type of sieve estimation where the basis functions are flexibly learned from the data. Neural networks are perhaps not as familiar to economists as other methods, and indeed, were out of favor in the machine learning community for several years, returning to prominence only very recently in the form of deep learning. Deep neural nets contain many hidden layers of neurons between the input and output layers, and have been found to exhibit superior performance across a variety of contexts. Our work aims to bring wider attention to these methods and to take the first step toward filling the gap in theoretical understanding of inference using deep neural networks. Our results can be used in many economic contexts, from selection models to games, from consumer surplus to dynamic discrete choice.

Before the recent surge in attention, neural networks had taken a back seat to other methods (such as kernel methods or forests) largely because of their modest empirical performance and challenging optimization. However, the availability of scalable computing and stochastic optimization techniques (LeCun, Bottou, Bengio, and Haffner, 1998; Kingma and Ba, 2014) and the change from smooth sigmoid-type activation functions to rectified linear units (ReLU), $x \mapsto \max(x, 0)$ (Nair and Hinton, 2010), have seemingly overcome optimization hurdles. Deep learning perform now matches or sets the state of the art in many prediction contexts (Krizhevsky, Sutskever, and Hinton, 2012; He, Zhang, Ren, and Sun, 2016). Our results speak directly to this modern implementation. We explicitly model the depth of the network as diverging with the sample size and focus on the ReLU activation function.

Further back in history, before falling out of favor, neural networks were widely studied and applied, particularly in the 1990s. In that time, *shallow* neural networks were shown to have many

good theoretical properties. Intuitively, neural networks are a form of sieve estimation, wherein basis functions of the original variables are used to approximate unknown nonparametric objects. What sets neural nets apart is that the basis functions are themselves learned from the data by optimizing over many flexible combinations of simple functions. It has been known for some time that such networks yield universal approximations (Hornik, Stinchcombe, and White, 1989). Comprehensive theoretical treatments are given by White (1992) and Anthony and Bartlett (1999). Of particular relevance in this strand of theoretical work is Chen and White (1999), where it was shown that single-layer, sigmoid-based networks could attain sufficiently fast rates for semiparametric inference (see Chen (2007) for more references).

We explicitly depart from these works by focusing on the modern setting of deep neural networks with the rectified linear (ReLU) activation function. We briefly review their construction in Section 2; for more see Goodfellow, Bengio, and Courville (2016). We provide nonasymptotic bounds for nonparametric estimation using deep neural networks, immediately implying convergence rates. The bounds and convergence rates appear to be new to the literature and are one of the main theoretical contributions of the paper. We provide results for the two most popular contexts, least squares and logistic regression, as concrete illustrations. Other nonparametric contexts (hazard models, generalized linear models) could be handled as well. Our proof strategy is novel: we employ a localization analysis that uses scale-insensitive measures of complexity, allowing us to consider richer classes of neural networks. This is in contrast to analyses which restrict the networks to have bounded parameters for each unit (discussed more below) and to the application of scale sensitive measures such as metric entropy (used by Chen and White, 1999, for example). These approaches would not deliver our sharp bounds and fast rates. Recent developments in approximation theory and complexity for deep ReLU networks are important building blocks for our results.

Our second main results give valid inference on finite-dimensional parameters following first-step estimation using deep nets. We focus on causal inference for illustration. Program evaluation with observational data is one of the most common and important inference problems, and has often been used as a first test case for theoretical study of inference following machine learning (e.g., Belloni, Chernozhukov, and Hansen, 2014; Farrell, 2015; Belloni, Chernozhukov, Fernández-Val, and Hansen, 2017; Athey, Imbens, and Wager, 2018). (Causal inference as a whole is a vast literature; see Imbens and Rubin (2015) for a broad review and Abadie and Cattaneo (2018) for

a recent review of program evaluation methods, and further references in both.) We give specific results for average treatment effects, expected utility/profits from treatment targeting strategies, and decomposition effects. Our results allow planners (e.g., firms or medical providers) to compare different strategies, either predetermined or estimated using auxiliary data, and recognizing that targeting can be costly, decide which strategy to implement. Other estimands are discussed briefly. Deep neural networks have been argued (experimentally) to outperform the previous state-of-the-art in causal inference (Westreich, Lessler, and Funk, 2010; Johansson, Shalit, and Sontag, 2016; Shalit, Johansson, and Sontag, 2017; Hartford, Lewis, Leyton-Brown, and Taddy, 2017). To the best of our knowledge, ours are among the first theoretical results that explicitly deliver inference using deep neural networks.

We focus on causal effect type parameters for concreteness and their wide applicability, as well as to allow direct comparison to the literature above, but our results are not limited to only these objects. In particular, our results yield inference on essentially any estimand that admits a locally robust estimator (Chernozhukov, Escanciano, Ichimura, Newey, and Robins, 2018) that depends only on conditional expectations (under appropriate regularity conditions). Our aim is not to innovate at the semiparametric step, for example by seeking weaker conditions on the first stage, but rather, we aim to utilize such results. Prior work has verified the high-level conditions for other first-stage estimators, such as traditional kernels or series/sieves, lasso methods, sigmoid-based shallow neural networks, and others (under suitable assumptions for each method). Our work contributes directly to this area of research by showing that deep nets are a valid and useful first-step estimator, in particular, attaining a rate of $o(n^{-1/4})$ under appropriate smoothness conditions. Using "overfitting" robust inference procedures (Cattaneo, Jansson, and Ma, 2018) may also be possible following deep learning, but is less obvious at present. Finally, we do not need to rely on sample splitting or cross fitting.

We numerically illustrate our results, and more generally the utility of deep learning, with a detailed simulation study and an empirical study of a direct mail marketing campaign. Our data come from a large US consumer products retailer and consists of close to three hundred thousand consumers with one hundred fifty covariates. This is the same data that was used by Hitsch and Misra (2018) to study various estimators, both traditional and modern, of heterogeneous treatment effects. We refer the reader to that paper for a more complete description of the data as well as

results using other estimators (see also Hansen, Kozbur, and Misra (2017)). We study the effect of catalog mailings on consumer purchases, and moreover, compare different targeting strategies (i.e. to which consumers catalogs should be mailed). The cost of sending out a single catalog can be close to one dollar, and with millions being set out, carefully assessing the targeting strategy is crucial. Our results suggest that deep nets are at least as good as (and sometimes better) that the best methods found by Hitsch and Misra (2018).

The remainder of the paper proceeds as follows. Next, we briefly review the related theoretical literature. Section 2 introduces deep ReLU networks and states our main theoretical results: nonasymptotic bounds and convergence rates for least squares and logistic regression. The semiparametric inference problem is set up in Section 3 and asymptotic results are presented in Section 4. The empirical application is presented in Section 5. Results of a simulation study are reported in Section 6. Section 7 concludes. All proofs are given in the appendix.

1.1 Related Theoretical Literature

Our paper contributes to several rapidly growing literatures, and we can not hope to do justice to each here. We give only those citations of particular relevance; more references can be found in these works. First, there has been much recent theoretical study of the properties of the machine learning tools, either as an end in itself or with an eye toward use in semiparametric inference. Much of this work has focused on the lasso and its variants (Bickel, Ritov, and Tsybakov, 2009; Belloni, Chernozhukov, and Wang, 2011; Belloni, Chen, Chernozhukov, and Hansen, 2012; Farrell, 2015) and tree/forest based methods (Wager and Athey, 2018), though earlier work studied shallow (typically with a single hidden layer) neural networks with smooth activation functions (White, 1989, 1992; Chen and White, 1999). We fill the gap in this literature by studying *deep* neural networks with the non-smooth ReLU activation.

A second, intertwined strand of literature focuses on inference following the use of machine learning methods, often with a focus on causal effects. Initial theoretical results were concerned obtaining valid inference on a coefficient in a high-dimensional regression, following model selection or regularization, with particular focus on the lasso (Belloni, Chen, Chernozhukov, and Hansen, 2012; Javanmard and Montanari, 2014; van de Geer, Buhlmann, Ritov, and Dezeure, 2014). Intuitively, this is a semiparametric problem, where the coefficient of interest is estimable at the

parametric rate, and the remaining coefficients are a nonparametric nuisance parameter estimated using machine learning methods. Building on this intuition, many have studied the semiparametric stage directly, such as obtaining novel, weaker conditions easing the application of machine learning methods (Belloni, Chernozhukov, and Hansen, 2014; Farrell, 2015; Chernozhukov, Escanciano, Ichimura, Newey, and Robins, 2018; Belloni, Chernozhukov, Chetverikov, Hansen, and Kato, 2018, and references therein). Conceptually related to this strand are targeted maximum likelihood (van der Laan and Rose, 2001) and the higher-order influence functions (Robins, Li, Tchetgen, and van der Vaart, 2008; Robins, Li, Mukherjee, Tchetgen, and van der Vaart, 2017). Our work builds on this work, employing conditions therein, and in particular, verifying them for deep ReLU nets.

Finally, our convergence rates build on, and contribute to, the recent theoretical machine learning literature on deep neural networks. Because of the renaissance in deep learning, a considerable amount of study has been done in recent years. Of particular relevance to us are Yarotsky (2017, 2018) and Bartlett, Harvey, Liaw, and Mehrabian (2017); a recent textbook treatment, containing numerous other references, is given by Goodfellow, Bengio, and Courville (2016).

2   Deep Neural Networks

In this section we will give our main theoretical results: nonasymptotic bounds and associated convergence rates for nonparametric regression using deep neural nets. The utility of these results for second-step semiparametric causal inference (the downstream task), for which our rates are sufficiently rapid, is demonstrated in Section 4. We view our results as an initial step in establishing both the estimation and inference theory for modern deep neural networks, i.e. those built using a multi-layer perceptron architecture (described below) and the nonsmooth ReLU activation function. This combination is crucial: it has demonstrated state of the art performance empirically and can be feasibly optimized. This is in contrast with sigmoid-based networks, either shallow (for which theory exists, but may not match empirical performance) or deep (which are not feasible to optimize), and with shallow ReLU networks, which are not known to approximate broad classes functions.

As neural networks are perhaps less familiar to economists and other social scientists, we first briefly review the construction of deep ReLU nets. Our main focus will be on the fully connected feedfoward neural network, frequently referred to as a multi-layer perceptron, as this is the most

commonly implemented network architecture and we want our results to inform empirical practice. However, our results are more general, accommodating other architectures provided they are able to yield a universal approximation (in the appropriate function class), and so we review neural nets more generally and give concrete examples.

The nonparametric setup we consider is standard. Our goal is to estimate an unknown smooth function $f_*(\boldsymbol{x})$, that relates the covariates $\boldsymbol{X} \in \mathbb{R}^d$ to a scalar outcome Y. We collect these random variables into the vector $\boldsymbol{Z} = (Y, \boldsymbol{X}')' \in \mathbb{R}^{d+1}$ and let a realization be $\boldsymbol{z} = (y, \boldsymbol{x}')'$. Accuracy is measured by a per-observation loss function denoted by $\ell(f, \boldsymbol{z})$. We cover both least squares and logistic regression as explicit examples. Both play a role in semiparametric inference on causal effects, in particular corresponding to the outcome and propensity score models, respectively. For least squares, the target function and loss are

$$f_*(\boldsymbol{x}) := \mathbb{E}[Y|\boldsymbol{X} = \boldsymbol{x}] \qquad \text{and} \qquad \ell(f, \boldsymbol{z}) = \frac{1}{2}(y - f(\boldsymbol{x}))^2, \tag{2.1}$$

respectively, while for logistic regression these are

$$f_*(\boldsymbol{x}) := \log \frac{\mathbb{E}[Y|\boldsymbol{X} = \boldsymbol{x}]}{1 - \mathbb{E}[Y|\boldsymbol{X} = \boldsymbol{x}]} \qquad \text{and} \qquad \ell(f, \boldsymbol{z}) = -yf(\boldsymbol{x}) + \log\left(1 + e^{f(\boldsymbol{x})}\right). \tag{2.2}$$

Other loss functions (with smoothness and curvature) can be accommodated; our results naturally extend to cases such as generalized linear models, for example multinomial logistic regression.

2.1 Neural Network Constructions

For either least squares or logistic loss, we estimate the target function using a deep ReLU network. We will give a brief outline of their construction here, paying closer attention to the details germane to our theory; complete introductions are given by Anthony and Bartlett (1999) and Goodfellow, Bengio, and Courville (2016).

The crucial choice is the specific network architecture, or class. In general we will call this $\mathcal{F}_{\text{DNN}}$. From a theoretical point of view, different classes have different complexity and different approximating power. We give results for several concrete examples below. We will focus on *feedforward neural networks* (Anthony and Bartlett, 1999). An example of a feedforward network
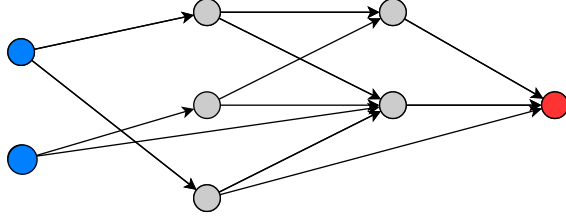
Figure 1: Illustration of a feedforward neural network with $W = 18$, $L = 2$, $U = 5$, and input dimension $d = 2$. The input units are shown in blue at left, the output in red at right, and the hidden units in grey between them.
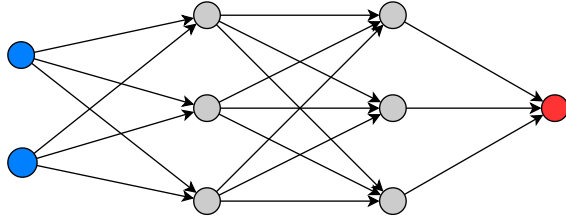

Figure 2: Illustration of multi-layer perceptron $\mathcal{F}_{\mathrm{MLP}}$ with $H = 3$, $L = 2$ ($U = 6$, $W = 25$), and input dimension $d = 2$.

is shown in Figure 1. The network consists of d input units, corresponding to the covariates $\boldsymbol{X} \in \mathbb{R}^d$, one output unit for the outcome Y. Between these are U hidden units, or computational nodes or neurons. These are connected by a directed acyclic graph specifying the architecture. The key graphical feature of a feedforward network is that hidden units are grouped in a sequence of L layers, the *depth* of the network, where a node is in layer $l = 1, 2, \ldots, L$, if it has a predecessor in layer $l-1$ and no predecessor in any layer $l' \geq l$. The *width* of the network at a given layer, denoted H_l, is the number of units in that layer. The network is completed with the choice of an *activation function* $\sigma : \mathbb{R} \mapsto \mathbb{R}$ applied to the output of each node as described below. In this paper, we focus on the popular ReLU activation function $\sigma(x) = \max(x, 0)$ (see also Remark 3).

An important and widely used subclass is the one that is *fully connected* between consecutive layers but has *no* other connections and each layer has number of hidden units that are of the same order of magnitude. This architecture is often referred to as a *Multi-Layer Perceptron* (MLP) and we denote the class as $\mathcal{F}_{\mathrm{MLP}}$. See Figure 2, cf. Figure 1. We will assume that all the width of all layers share a common asymptotic order H, implying that for this class $U \asymp LH$.

We will allow for generic feedforward networks in our results, but we present special results for the MLP case, as it is widely used in empirical practice. As we will see below, the architecture, through its complexity, and more importantly, approximation power, plays a crucial role in the

7

final convergence rate. In particular, at present we find only a suboptimal rate for the MLP case, but our upper bound is still sufficient for semiparametric inference. (As a note on exposition, while our main results are in fact nonasymptotic bounds that hold with high probability, for simplicity we will refer to our results as "rates" in most discussion.)

To build intuition on the computation, and compare to other nonparametrics methods, let us for now focus on least squares (2.1) with a continuous outcome using a multilayer perceptron with constant width H. Each hidden unit u receives an input in the form of a linear combination $\tilde{\boldsymbol{x}}'\boldsymbol{w}+b$, and then returns $\sigma(\tilde{\boldsymbol{x}}'\boldsymbol{w}+b)$, where the vector $\tilde{\boldsymbol{x}}$ collects the output of all the units with a directed edge into u (i.e., from prior layers). The final layer's output is $\tilde{\boldsymbol{x}}'\boldsymbol{w}+b$. The parameters to be optimized are the weight vector $\boldsymbol{w}$ and the constant term b, with one set for each node of the graph. (The constant term is often referred to as the "bias" in the networks literature, but given the loaded meaning of this term in inference, we will avoid referring to b as a bias.) The collection, over all nodes, of $\boldsymbol{w}$ and b, constitutes the parameters θ which are optimized in the final estimation. We denote W as the total number of parameters (both weights and biases) of the network. For the MLP $W = (d+1)H + (L-1)(H^2 + H) + H + 1$.

Optimization proceeds layer-by-layer using (variants of) stochastic gradient descent, with gradients of the parameters calculated by back-propagation (implementing the chain-rule) induced by the network structure. To see this, let the output of a node $u = (h,l)$, for $h = 1,\ldots H$, $l = 1,\ldots L$, be denoted by the scalar $\tilde{x}_{h,l}$. This is computed as $\tilde{x}_{h,l} = \sigma(\tilde{\boldsymbol{x}}'_{l-1}\boldsymbol{w}_{h,l-1} + b_{h,l-1})$, where $\tilde{\boldsymbol{x}}_{l-1} = (\tilde{x}_{1,l-1}, \ldots, \tilde{x}_{H,l-1})'$. The final output is $\hat{y} = \tilde{\boldsymbol{x}}'_L\boldsymbol{w}_L + b_L$. Once we recall that $\tilde{\boldsymbol{x}}_L = \tilde{\boldsymbol{x}}_L(\boldsymbol{x})$, we can view this as a basis function expansion (albeit a complex one) of the original observation $\boldsymbol{x}$, and then the form $\hat{f}_{\mathrm{MLP}}(\boldsymbol{x}) = \tilde{\boldsymbol{x}}_L(\boldsymbol{x})'\boldsymbol{w}_L + b_L$ is reminiscent of a traditional series (linear sieve) estimator. If all layers save the last were fixed, we could simply optimize using least squares directly: $(\boldsymbol{w}_L, b_L) = \arg\min_{\boldsymbol{w},b} \|y_i - \tilde{\boldsymbol{x}}'_L\boldsymbol{w} - b\|^2_n$.

The crucial distinction is of course that the set of basis functions $\tilde{\boldsymbol{x}}_L(\cdot)$ is learned from the data. The "basis" is $\tilde{\boldsymbol{x}}_L = (\tilde{x}_{1,L}, \ldots, \tilde{x}_{H,L})'$, where each $\tilde{x}_{h,L} = \sigma(\tilde{\boldsymbol{x}}'_{L-1}\boldsymbol{w}_{h,L-1} + b_{h,L-1})$. Therefore, "before" we can solve the least squares problem above, we would have to estimate $(\boldsymbol{w}'_{h,L-1}, b_{h,L-1})$, $h = 1,\ldots,H$, anticipating the final estimation. These in turn depend on the prior layer, and so forth back to the original inputs $\boldsymbol{X}$. Measuring the gradient of the loss with respect to each layer of parameters uses the chain rule recursively, and is implemented by back propagation. This is sim-

ply a sketch of course; for further introduction, see Hastie, Tibshirani, and Friedman (2009) and Goodfellow, Bengio, and Courville (2016).

To further clarify the use of deep nets, it is useful to make explicit analogies to more classical nonparametric techniques, leveraging the form $\hat{f}_{\text{MLP}}(\boldsymbol{x}) = \tilde{\boldsymbol{x}}_L(\boldsymbol{x})'\boldsymbol{w}_L + b_L$. For a traditional series estimator, say smoothing splines, the two choices for the practitioner are the spline basis (the shape and the degree) and the number of terms (knots), commonly referred to as the smoothing and tuning parameters, respectively. In kernel regression, these would respectively be the shape of the kernel (and degree of local polynomial) and the bandwidth(s). For neural networks, the same phenomena are present: the architecture as a *whole* (the graph structure and activation function) are the smoothing parameters while the width and depth play the role of tuning parameters for a set architecture.

The architecture plays a crucial role in that it determines the approximation power of the network, and it is worth noting that because of the relative complexity of neural networks, such approximations, and comparisons across architectures, are not simple. It is comparatively obvious that quartic splines are more flexible than cubic splines (for the same number of knots) as is a higher degree local polynomial (for the same bandwidth). At a glance, it may not be clear what function class a given network architecture (width, depth, graph structure, and activation function) can approximate. As we will show below, the MLP architecture is not yet known to yield an optimal approximation (for a given width and depth) and therefore we are only able to prove a bound with slower than optimal rate. As a final note, computational considerations are important for deep nets in a way that is not true conventionally. See Remarks 1, 2, and 3.

Just as for classical nonparametrics, for a fixed architecture, it is the tuning parameter choices that determine the rate of convergence (for a fixed smoothness of the underlying function). The new wave of study of neural networks, focusing on depth, is in its infancy theoretically. As such, there is no understanding yet of optimal architecture(s) or tuning parameters. Choices of both are quite difficult, and only preliminary research has been done (e.g., Daniely, 2017; Telgarsky, 2016; Safran and Shamir, 2016; Mhaskar and Poggio, 2016a; Raghu, Poole, Kleinberg, Ganguli, and Sohl-Dickstein, 2017, and references therein). Further exploration of these ideas is beyond the current scope. It is interesting to note that in some cases, a good approximation can be obtained even with a fixed width H, provided the network is deep enough, a very particular way of enriching

the "sieve space" $\mathcal{F}_{\text{DNN}}$. See Corollary 2.

In sum, for a user-chosen architecture $\mathcal{F}_{\text{DNN}}$, encompassing the choices $\sigma(\cdot)$, U, L, W, and the graph structure, the final estimate is computed using observed samples $\boldsymbol{z}_i = (y_i, \boldsymbol{x}_i')'$, $i = 1, 2, \ldots, n$, of $\boldsymbol{Z}$, by solving

$$\widehat{f}_{\text{DNN}} := \underset{\substack{f_\theta \in \mathcal{F}_{\text{DNN}} \\ \|f_\theta\|_\infty \leq 2M}}{\arg\min} \sum_{i=1}^{n} \ell\left(f, \boldsymbol{z}_i\right). \tag{2.3}$$

When (2.3) is restricted to the MLP class we denote the resulting estimator $\widehat{f}_{\text{MLP}}$. The choice of M may be arbitrarily large, and is part of the definition of the class $\mathcal{F}_{\text{DNN}}$. This is neither a tuning parameter nor regularization in the usual sense: it is not assumed to vary with n, and beyond being finite, no properties of M are required. This is simply a formalization of the requirement that the optimizer is not allowed to diverge on the function level in the l_∞ sense — the weakest form of constraint. It is important to note that while typically regularization will alter the approximation power of the class, that is not the case with the choice of M as we will assume that the true function $f_*(\boldsymbol{x})$ is bounded, as is standard in nonparametric analysis. With some extra notational burden, one can make the dependence of the bound on M explicit, though we omit this for clarity as it is not related to statistical issues.

Remark 1. In applications it is common to apply some form of regularization to the optimization of (2.3). However, in theory, the role of explicit regularization is unclear and may be unnecessary, as stochastic gradient descent presents good, if not better, solutions empirically (see Section 6 and Zhang, Bengio, Hardt, Recht, and Vinyals, 2016). Regularization may improve empirical performance in low signal-to-noise ratio problems. A detailed investigation is beyond the scope of the current work, though we do investigate this numerically in Sections 5 and 6. There are many alternative regularization methods, including L_1 and L_2 (weight decay) penalties, drop out, and others. ⌟

2.2 Bounds and Convergence Rates for Multi-Layer Perceptrons

We can now state our first theoretical results: bounds and convergence rates for deep ReLU networks. All proofs appear in Appendix A. We study neural networks from a nonparametric point

of view (e.g., White, 1989, 1992; Schmidt-Hieber, 2017; Liang, 2018; Bauer and Kohler, 2017, in specific scenarios). Chen and Shen (1998) and Chen and White (1999) share our goal, fast convergence rates for use in semiparametric inference, but focus on shallow, sigmoid-based networks compared to our deep, ReLU-based networks, though they consider dependent data which we do not. Our theoretical approach is quite different. In particular, Chen and White (1999) obtain sufficiently fast rates by following the approach of Barron (1993) in using Maurey's method (Pisier, 1981) for approximation, but applying the refinement of Makovoz (1996). Our analysis of deep nets instead employs localization methods (Koltchinskii and Panchenko, 2000; Bartlett, Bousquet, Mendelson, et al., 2005; Koltchinskii, 2006; Liang, Rakhlin, and Sridharan, 2015), along with the recent approximation work of Yarotsky (2017, 2018) and complexity results of Bartlett, Harvey, Liaw, and Mehrabian (2017).

The regularity conditions we require are collected in the following.

Assumption 1. *Assume that $\boldsymbol{z}_i = (y_i, \boldsymbol{x}_i')', 1 \leq i \leq n$ are i.i.d. copies of $\boldsymbol{Z} = (Y, \boldsymbol{X}) \in \mathcal{Y} \times [-1, 1]^d$, where X is continuously distributed. For an absolute constant $M > 0$, assume $\|f_*\|_\infty \leq M$ and either $f_*(\boldsymbol{x}) = \mathbb{E}[Y \mid \boldsymbol{X} = \boldsymbol{x}]$ and $\mathcal{Y} = [-M, M]$ or $f_*(\boldsymbol{x}) = \log\left(\mathbb{E}[Y|\boldsymbol{X} = \boldsymbol{x}]/(1 - \mathbb{E}[Y|\boldsymbol{X} = \boldsymbol{x}])\right)$ and $\mathcal{Y} = \{0, 1\}$.*

This assumption is fairly standard in nonparametrics. The only restriction worth mentioning is that for least squares regression we assume that the outcome is bounded. In common practice our restriction is not substantially more limiting than the usual assumption of a model such as $Y = f_*(\boldsymbol{X}) + \varepsilon$, where $\boldsymbol{X}$ is compact-supported, f_* is bounded, and the stochastic error ε possesses many moments. Indeed, in many applications such a structure is only coherent with bounded outcomes, such as the common practice of including lagged outcomes as predictors. The assumption of continuously distributed covariates is quite standard. From a theoretical point of view, covariates taking on only a few values can be conditioned on and then averaged over, and these will, as usual, not enter into the dimensionality which curses the rates. Discrete covariates taking on many values may be more realistically thought of as continuous, and it may be more accurate to allow these to slow the convergence rates. Our focus on $L_2(X)$ convergence allows for these essentially automatically. Finally, from a practical point of view, deep networks handle discrete covariates seamlessly and have demonstrated excellent empirical performance, which is in contrast to other

more classical nonparametric techniques that may require more manual adaptation.

We begin with the most important network architecture, the multi-layer perceptron. This is the most widely used network architecture in practice and an important contribution of our work is to cover this directly, along with ReLU activation. MLPs are known now to approximate smooth functions well, leading to our next assumption: that the target function f_* lies in a Sobolev ball with certain smoothness.

Assumption 2. *Assume f_* lies in the Sobolev ball $\mathcal{W}^{\beta,\infty}([-1,1]^d)$, with smoothness $\beta \in \mathbb{N}_+$,*

$$f_*(x) \in \mathcal{W}^{\beta,\infty}([-1,1]^d) := \left\{ f : \max_{\alpha,|\alpha|\leq\beta} \operatorname*{ess\,sup}_{x\in[-1,1]^d} |D^\alpha f(x)| \leq 1 \right\},$$

where $\alpha = (\alpha_1, \ldots, \alpha_d)$, $|\alpha| = \alpha_1 + \ldots + \alpha_d$ and $D^\alpha f$ is the weak derivative.

Under Assumptions 1 and 2 we obtain the following result, which, to the best of our knowledge, is new to the literature. In some sense, this is our main result for deep learning, as it deals with the most common architecture. We apply this in Sections 4 and 5 for semiparametric inference.

Theorem 1 (Multi-Layer Perceptron)**.** *Suppose Assumptions 1 and 2 hold. Let $\widehat{f}_{\mathrm{MLP}}$ be the deep ReLU network estimator defined by (2.3), restricted to $\mathcal{F}_{\mathrm{MLP}}$, for either least squares (2.1) or logistic (2.2) loss, with $H_n \asymp n^{\frac{d}{2(\beta+d)}} \log^2 n$ and $L_n \asymp \log n$. Then with probability at least $1 - \exp(-n^{\frac{d}{\beta+d}} \log^8 n)$,*

(a) $\|\widehat{f}_{\mathrm{MLP}} - f_*\|_{L_2(X)}^2 \leq C \cdot \left\{ n^{-\frac{\beta}{\beta+d}} \log^8 n + \dfrac{\log\log n}{n} \right\}$ *and*

(b) $\mathbb{E}_n\left[(\widehat{f}_{\mathrm{MLP}} - f_*)^2 \right] \leq C \cdot \left\{ n^{-\frac{\beta}{\beta+d}} \log^8 n + \dfrac{\log\log n}{n} \right\},$

for a universal constant $C > 0$ independent of n.

The proof of this result is in the Appendix. However, several aspects warrant discussion. We build on the recent results of Bartlett, Harvey, Liaw, and Mehrabian (2017), who find nearly-tight bounds on the Vapnik-Chervonenkis (VC) dimension of deep nets. One contribution of our proof is to derive a *scale sensitive* localization theory with *scale insensitive* measures, such as VC- or Pseudo-dimension, for deep neural networks. This has two tangible benefits. First, we do not restrict the class of network architectures to have bounded weights for each unit (scale insensitive),

in accordance to standard practice (Zhang, Bengio, Hardt, Recht, and Vinyals, 2016). Moreover, this allows for a richer set of approximating possibilities, in particular allowing more flexibility in seeking architectures with specific properties, as we explore in the next subsection. This is in contrast to the classic sieve analysis with scale sensitive measure such as metric entropy. Second, from a technical point of view, we are able to attain a faster rate on the second term of the bound, order n^{-1} in the sample size, instead of the $n^{-1/2}$ that would result from a direct application of uniform deviation bounds. This upper bound informs the trade offs between H_n and L_n, and the approximation power, and may point toward optimal architectures for statistical inference.

This result gives a nonasymptotic bound that holds with high probability. As mentioned above, we will generally refer to our results simply as "rates" when this causes no confusion. This result relies on choosing H_n appropriately given the smoothness β of Assumption 2. Of course, the true smoothness is unknown and thus in practice the "β" appearing in H_n, and consequently in the convergence rates, need not match that of Assumption 2. In general, the rate will depend on the smaller of the two. Most commonly it is assumed that the user-chosen β is fixed and that the truth is smoother; witness the ubiquity of cubic splines and local linear regression. Rather than spell out these consequences directly, we will tacitly assume the true smoothness is not less than the β appearing in H_n (here and below). Adaptive approaches, as in classical nonparametrics, may also be possible with deep nets, but are beyond the scope of this study.

Even with these choices of H_n and L_n, the bound of Theorem 1 is not optimal (for fixed β, in the sense of Stone (1982)). We rely on the explicit approximating constructions of Yarotsky (2017), and it is possible that in the future improved approximation properties of MLPs will be found, allowing for a sharpening of Theorem 1 without substantive change to the argument. At present, it is not clear if this rate can be improved, but it is sufficiently fast for valid inference.

2.3 Other Network Architectures

Theorem 1 covers only one specific architecture, albeit the most important one at present. However, given that this field is rapidly evolving, it is important to consider other possible architectures which may be beneficial in some cases. To this end, we will state a more generic result and then two specific examples: one to obtain an faster rate of convergence and one for fixed-width networks. All of these results are, at present, more of theoretical interest than practical value, as they are

either agnostic about the network (thus infeasible) or rely on more limiting assumptions.

In order to be agnostic about the specific architecture of the network we need to be flexible in the approximation power of the class. To this end, we will replace Assumption 2 with the following generic assumption, rather more of a definition, regarding the approximation power of the network.

Assumption 3. *Let f_* lie in a class $\mathcal{F}$. For the feedforward network class $\mathcal{F}_{\mathrm{DNN}}$, used in* (2.3), *the approximation error ϵ_{DNN} is*

$$\epsilon_{\mathrm{DNN}} := \sup_{\substack{f_* \in \mathcal{F}}} \inf_{\substack{f \in \mathcal{F}_{\mathrm{DNN}} \\ \|f\|_\infty \leq 2M}} \|f - f_*\|_\infty \ .$$

It may be possible to require only an approximation in the $L_2(X)$ norm, but this assumption matches the current approximation theory literature and is more comparable with other work in nonparametrics, and thus we maintain the uniform definition.

Under this condition we obtain our the following generic result.

Theorem 2 (General Feedforward Architecture). *Suppose Assumptions 1 and 3 hold. Let $\widehat{f}_{\mathrm{DNN}}$ be the deep ReLU network estimator defined by* (2.3), *for either least squares* (2.1) *or logistic* (2.2) *loss. Then with probability at least $1 - e^{-\gamma}$,*

(a) $\|\widehat{f}_{\mathrm{DNN}} - f_*\|_{L_2(X)}^2 \leq C \left(\dfrac{W_n L_n \log U_n}{n} \log n + \dfrac{\log \log n + \gamma}{n} + \epsilon_{\mathrm{DNN}}^2 \right)$ *and*

(b) $\mathbb{E}_n \left[(\widehat{f}_{\mathrm{DNN}} - f_*)^2 \right] \leq C \left(\dfrac{W_n L_n \log U_n}{n} \log n + \dfrac{\log \log n + \gamma}{n} + \epsilon_{\mathrm{DNN}}^2 \right),$

for a universal constant $C > 0$ independent of n.

This result covers the general deep ReLU network problem defined in (2.3) for general feedforward architectures. The same comments as were made following Theorem 1 apply here as well: the same localization argument is used with the same benefits. We explicitly use this in the next two corollaries, where we exploit the allowed flexibility in controlling ϵ_{DNN} by stating results for particular architectures. The bound here is not directly applicable without specifying the network structure, which will determine both the variance portion (through W_n, L_n, and U_n) and the approximation error. With these set, the bound becomes operational upon choosing γ, which can be optimized as desired, and this will immediately then yield a convergence rate.

Turning to special cases, we first show that the optimal rate of Stone (1982) can be attained, up to log factors. However, this relies on a rather artificial network structure, designated to approximate functions in a Sobolev space well, but without concern for practical implementation. Thus, while the following rate improves upon Theorem 1, we view this result as mainly of theoretical interest: establishing that (certain) deep ReLU networks are able to attain the optimal rate.

Corollary 1 (Optimal Rate). *Suppose Assumptions 1 and 2 hold. Let $\widehat{f}_{\mathrm{OPT}}$ solve (2.3) using the (deep and wide) network of Yarotsky (2017, Theorem 1), with $W_n \asymp U_n \asymp n^{\frac{d}{2\beta+d}} \log n$ and $L_n \asymp \log n$, the following hold with probability at least $1 - e^{-\gamma}$,*

(a) $\|\widehat{f}_{\mathrm{OPT}} - f_*\|_{L_2(X)}^2 \leq C \cdot \left\{ n^{-\frac{2\beta}{2\beta+d}} \log^4 n + \frac{\log\log n + \gamma}{n} \right\}$ *and*

(b) $\mathbb{E}_n\left[(\widehat{f}_{\mathrm{OPT}} - f_*)^2 \right] \leq C \cdot \left\{ n^{-\frac{2\beta}{2\beta+d}} \log^4 n + \frac{\log\log n + \gamma}{n} \right\},$

for a universal constant $C > 0$ independent of n.

Next, we turn to *very* deep networks that are very narrow, which have attracted substantial recent interest. Theorem 1 and Corollary 1 dealt with networks where the depth and the width grow with sample size. This matches the most common empirical practice, and is what we use in Sections 5 and 6. However, it is possible to allow for networks of *fixed* width, provided the depth is sufficiently large. Using recent results (Mhaskar and Poggio, 2016b; Hanin, 2017; Yarotsky, 2018) we can establish the following result for very deep MLPs.

Corollary 2 (Fixed Width Networks). *Let the conditions of Theorem 1 hold, with $\beta \geq 1$ in Assumption 2. Let $\widehat{f}_{\mathrm{FW}}$ solve (2.3) for an MLP with $H = 2d + 10$ and $L \asymp n^{\frac{d}{2(2+d)}}$. Then with probability at least $1 - e^{-\gamma}$,*

(a) $\|\widehat{f}_{\mathrm{FW}} - f_*\|_{L_2(X)}^2 \leq C \cdot \left\{ n^{-\frac{2}{2+d}} \log^2 n + \frac{\log\log n + \gamma}{n} \right\}$ *and*

(b) $\mathbb{E}_n\left[(\widehat{f}_{\mathrm{FW}} - f_*)^2 \right] \leq C \cdot \left\{ n^{-\frac{2}{2+d}} \log^2 n + \frac{\log\log n + \gamma}{n} \right\},$

for a universal constant $C > 0$ independent of n.

This result is again mainly of theoretical interest. The class is only able to approximate well functions with $\beta = 1$ (cf. the choice of L) which limits the potential applications of the result

because, in practice, d will be large enough to render this rate, unlike those above, too slow for use in later inference procedures. In particular, if $d \geq 3$, the sufficient conditions of Theorem 3 fail.

Remark 2. Although there has been a great deal of work in easing implementation (optimization and tuning) of deep nets, it still may be a challenge in some settings, particularly when using non-standard architectures. See also Remark 1. Given the renewed interest in deep networks, this is an area of study already (Hartford, Lewis, Leyton-Brown, and Taddy, 2017; Polson and Rockova, 2018) and we expect this to continue and that implementations will rapidly evolve. This is perhaps another reason that Theorem 1 is, at the present time, the most practically useful.   ⌐

Remark 3. In principle, similar rates of convergence could be attained for other activation functions, given results on their approximation error. However, it is not clear what practical value would be offered due to computational issues (in which the activation choice plays a crucial role). Indeed, the recent switch to ReLU stems not from their greater approximation power, but from the fact that optimizing a deep net with sigmoid-type activation is unstable or impossible in practice. Thus, while it is certainly possible that we could complement the single-layer results with rates for sigmoid-based deep networks, these results would have no consequences for real-world practice. It is for these reasons that we focus on ReLU networks and also that we present both generic results and specific corollaries for different architectures.

From a purely practical point of view, several variations of the ReLU activation function have been proposed recently (including the so-called Leaky ReLU, Randomized ReLU, (Scaled) Exponential Linear Units, and so forth) and have been found in some experiments to improve optimization properties. It is not clear what theoretical properties these activation functions have or if the computational benefits persist more generically, though this area is rapidly evolving. We conjecture that our results could be extended to include these activation functions.   ⌐

3   Parameters of Interest

We will use the results above, in particular Theorem 1, coupled with results in the semiparametric literature, to deliver valid asymptotic inference for causal effects. The novelty of our results is not in this semiparametric stage per se, but rather in delivering valid inference after relying on deep

learning for the first step estimation. In this section we define the parameters of interest, while asymptotic inference is discussed next.

We will focus, for concreteness, on causal parameters that are of interest across in different disciplines: average treatment effects, expected utility (or profits) under different targeting policies, average effects on (non-)treated subpopulations, and decomposition effects. Our focus on causal inference with observational data is due to the popularity of these estimands both in applications and in theoretical work, thus allowing our results to be put to immediate use and easily compared to prior literature. The average treatment effect in particular is often used as a benchmark parameter for inference inference following machine learning (see Section 1.1). However, armed with our results for deep neural networks we can cover a great deal more (some discussion is in Section 3.4).

The estimation of average causal effects is a well-studied problem, and we will give only a brief overview here. Recent reviews and further references are given by Belloni, Chernozhukov, Fernández-Val, and Hansen (2017); Athey, Imbens, Pham, and Wager (2017); Abadie and Cattaneo (2018). We consider the standard setup for program evaluation with observational data: we observe a sample of n units, each exposed to a binary treatment, and for each unit we observe a vector of pre-treatment covariates, $\boldsymbol{X} \in \mathbb{R}^d$, treatment status $T \in \{0,1\}$, and a scalar post-treatment outcome Y. The observed outcome obeys $Y = TY(1) + (1-T)Y(0)$, where $Y(t)$ is the (potential) outcome under treatment status $t \in \{0,1\}$. The "fundamental problem" is that only $Y(0)$ or $Y(1)$ is observed for each unit, never both.

The crucial identification assumptions, which pertains to all the parameters we consider, are selection on observables, also known as ignorability, unconfoundedness, missingness at random, or conditional independence, and overlap, or common support. Let $p(\boldsymbol{x}) = \mathbb{P}[T = 1 | \boldsymbol{X} = \boldsymbol{x}]$ denote the propensity score and $\mu_t(\boldsymbol{x}) = E[Y(t) | \boldsymbol{X} = \boldsymbol{x}]$, $t \in \{0,1\}$ denote the two regression functions. We then assume the following throughout. Beyond this, we will mostly need only regularity conditions for inference.

Assumption 4. *For $t \in \{0,1\}$ and almost surely $\boldsymbol{X}$, $\mathbb{E}[Y(t)|T, \boldsymbol{X} = \boldsymbol{x}] = \mathbb{E}[Y(t)|\boldsymbol{X} = \boldsymbol{x}]$ and $\bar{p} \le p(\boldsymbol{x}) \le 1 - \bar{p}$ for some $\bar{p} > 0$.*

It will be useful to divide our discussion between parameters that are fully marginal averages, such as the average treatment effect, and those which are for specific subpopulations. Here, "sub-

populations" refer to the treated or nontreated groups, with corresponding parameters such as the treatment effect for the treated. Any parameter, in either case, can be studied for a suitable subpopulation defined by the covariates $\boldsymbol{X}$, such as a specific demographic group. Though causal effects as a whole share some structure, there are slight conceptual and notational differences. In particular, the form of the efficient influence function and doubly robust estimator is different for the two sets, but common within.

3.1 Full-Population Average Effect Parameters

Here we are interested in averages over the entire population. The prototypical parameter of interest is the average treatment effect:

$$\tau = \mathbb{E}[Y(1) - Y(0)]. \tag{3.1}$$

In the context of our empirical example, the treatment is being mailed a catalog and the outcome is either a binary purchase decision or dollars spent. The average treatment effect, also referred to as "lift" in digital contexts, corresponds to the expected gain in revenue from an average individual receiving the catalog compared to the same person not receiving the catalog.

A closely related parameter of interest is the average realized outcome, which in general may be interpreted as the expected utility or welfare from a treatment policy. In the context of our empirical application this is expected profits; in a medical context it would be the total health outcome. The question of interest here is whether a change in the treatment policy would be beneficial in terms of increasing outcomes, and this is judged using observational data. Intuitively, the average treatment effect is the expected gain from treatment for the "next" person exposed to treatment, relative to if they had not been exposed. That is, it is the expected change in the outcome. Expected utility/profit, on the other hand, is concerned with the total outcome, not the difference in outcomes. In the context of our empirical application, we are interested in the probability of making a purchase decision or in total sales, rather than the change in each. Our discussion is grounded in this language for easy comparison.

The parameter depends on a hypothetical treatment targeting strategy, which is often the object of evaluation. This is simply a rule that assigns a given set of characteristics (e.g. a consumer profile), determined by the covariates X, to treatment status: that is, a known function (which

may include randomization but is not estimated from the sample) $s(x) : \text{supp}\{\boldsymbol{X}\} \mapsto \{0, 1\}$. Note well that this is *not* necessarily the observed treatment: $s(\boldsymbol{x}_i) \neq t_i$. The policy maker may wish to evaluate the gain from targeting only a certain subset of customers, a price discrimination strategy, or comparisons of different such policies.

The parameter of interest is then then expected utility, or profit, from a fixed policy, given by

$$\pi(s) = \mathbb{E}\big[s(\boldsymbol{X})Y(1) + (1 - s(\boldsymbol{X}))\,Y(0)\big], \tag{3.2}$$

where we make explicit the dependence on the policy $s(\cdot)$. Compare to Equation (3.1) and recall that the *observed* outcome obeys $Y = TY(1) + (1 - T)Y(0)$. Whereas τ is the gain in assigning the next person to treatment and is given by the difference in potential outcomes, $\pi(s)$ is the expected outcome that would be observed for the next person if the treatment rule were $s(\boldsymbol{x})$.

A natural question is whether a candidate targeting strategy, say $s'(\boldsymbol{x})$, is superior to baseline or status quo policy, $s_0(\boldsymbol{x})$. This amounts to testing the hypothesis $H_0 : \pi(s') \geq \pi(s_0)$. To evaluate this, we can study the difference in expected profits, which amounts to

$$\pi(s', s_0) = \pi(s') - \pi(s_0) = \mathbb{E}\big[(s'(\boldsymbol{X}) - s_0(\boldsymbol{X}))Y(1) + \big(s_0(\boldsymbol{X}) - s'(\boldsymbol{X})\big)Y(0)\big]. \tag{3.3}$$

Assumption 4 provides identification for $\pi(s)$ and $\pi(s', s_0)$, arguing analogously as for τ. Moreover, notice that $\pi(s', s_0) = \mathbb{E}[(s'(\boldsymbol{X}) - s_0(\boldsymbol{X}))(Y(1) - Y(0))] = \mathbb{E}[(s'(\boldsymbol{X}) - s_0(\boldsymbol{X}))\tau(\boldsymbol{X})]$, where $\tau(\boldsymbol{x}) = \mathbb{E}[Y(1) - Y(0) \mid \boldsymbol{X} = \boldsymbol{x}]$ is the conditional average treatment effect. The latter form makes clear that only those differently treated, of course, impact the evaluation of s' compared to s_0. The strategy s' will be superior if, on average, it targets those with a higher individual treatment effect, $\tau(\boldsymbol{x})$. Estimating the optimal treatment policy from the data is discussed briefly in Section 3.3.

The common structure of these parameters is that they all involve full-population averages of the potential outcomes, possibly scaled by a known function. For these parameters, the influence function is known from Hahn (1998), and estimators based on the influence function are doubly robust, as they remain consistent if either the regression functions or the propensity score are correctly specified (Robins, Rotnitzky, and Zhao, 1994, 1995). With a slight abuse of terminology (since we are omitting the centering), the influence function for a single average potential outcome,

19

$t \in \{0, 1\}$, is given by, for $\boldsymbol{z} = (y, t, \boldsymbol{x}')'$,

$$\psi_t(\boldsymbol{z}) = \frac{\mathbb{1}\{T = t\}(y - \mu_t(\boldsymbol{x}))}{\mathbb{P}[T = t \mid \boldsymbol{X} = \boldsymbol{x}]} + \mu_t(\boldsymbol{x}). \tag{3.4}$$

Our estimation of τ, $\pi(s)$, and $\pi(s', s_0)$ will utilize sample averages of this function, with unknown objects replaced by estimators. Our use of influence functions here follows the recent literature in econometrics showing that the double robustness implies valid inference under weaker conditions on the first step nonparametric estimates (Farrell, 2015; Chernozhukov, Chetverikov, Demirer, Duflo, Hansen, Newey, and Robins, 2018).

3.2   Subpopulation Effect Parameters

The second type of causal effects of interest are based on potential outcomes averaged over only a specific treatment group. A single such average, for $t, t' \in \{0, 1\}$, is denoted by

$$\rho_{t,t'} = \mathbb{E}[Y(t) \mid T = t']. \tag{3.5}$$

Many interesting parameters are linear combinations of these for different t and t'. We focus on two for concreteness. (We could also consider averages restricted by targeting-type functions, as in expected utility/profit, but for brevity we omit this.) The most well-studied of these parameters is the treatment effect on the treated, given by

$$\tau_{1,0} = \mathbb{E}[Y(1) - Y(0) \mid T = 1] = \rho_{1,1} - \rho_{0,1}. \tag{3.6}$$

To appreciate the breadth of this framework, and the applicability of our causal inference results, we also consider a decomposition parameter, a semiparametric analogue of Oaxaca-Blinder (Kitagawa, 1955; Oaxaca, 1973; Blinder, 1973). In this context, the "treatment" variable T is typically not a treatment assignment per se, but rather an exogenous covariate such as a demographic indicator, perhaps most commonly a male/female indicator. See Fortin, Lemieux, and Firpo (2011) for a complete discussion and further references. The parameter of interest in this case is the decomposition of $\Delta = \mathbb{E}[Y(1) \mid T = 1] - \mathbb{E}[Y(0) \mid T = 0]$, into the difference in the covariate distributions and the difference in expected outcomes. These can be written as functions of different $\rho_{t,t'}$. For

example, $\Delta_X = \mathbb{E}[Y(1)|T=1] - \mathbb{E}[Y(1)|T=0] = \mathbb{E}[\mu_1(\boldsymbol{X})|T=1] - \mathbb{E}[\mu_1(\boldsymbol{X})|T=0] = \rho_{1,1} - \rho_{1,0}$. We are in general interested in

$$\Delta = \Delta_X + \Delta_\mu, \qquad \Delta_X = \rho_{1,1} - \rho_{1,0}, \qquad \text{and} \qquad \Delta_\mu = \rho_{1,0} - \rho_{0,0}. \qquad (3.7)$$

Just as in the case of full-population averages, the influence function is known and leads to a doubly robust estimator. For a single $\rho_{t,t'}$, the (uncentered) influence function is (cf. (3.4)):

$$\psi_{t,t'}(\boldsymbol{z}) = \frac{\mathbb{P}[T=t' \mid \boldsymbol{X}=\boldsymbol{x}]}{\mathbb{P}[T=t']} \frac{\mathbb{1}\{T=t\}(y - \mu_t(\boldsymbol{x}))}{\mathbb{P}[T=t \mid \boldsymbol{X}=\boldsymbol{x}]} + \frac{\mathbb{1}\{T=t'\}\mu_t(\boldsymbol{x})}{\mathbb{P}[T=t']}. \qquad (3.8)$$

Estimation and inference requires, as above, estimation of the propensity scores and regression functions, depending on the exact choices of t and t', and here we also require the marginal probability of treatments.

3.3 Optimal Policies

Moving beyond inference on a fixed parameter, our results on deep neural networks can be used to address optimal targeting. In the notation of Section 3.1, this amounts to finding a policy, say $s_\star(\boldsymbol{x})$, that maximizes a given measure of utility stemming from treatment, generally the expected gain relative to a baseline policy. In Section 3.1 we considered inference on the utility (or profit) difference between two given strategies, a candidate $s'(\boldsymbol{x})$ and a baseline $s_0(\boldsymbol{x})$. Now, we turn from inference to using the data to find the $s_\star(\boldsymbol{x})$ which maximizes this gain. This problem has been widely studied in econometrics and statistics; for detailed discussion and numerous references see Manski (2004), Hirano and Porter (2009), Kitagawa and Tetenov (2018), and Athey and Wager (2018). In particular, the latter noticed using the locally robust framework allows policy optimization under nearly the same conditions as inference and proved fast convergence rates of the estimated policy in terms of regret.

More formally, we want to find the optimal choice $s_\star(\boldsymbol{x})$ in some policy/action space $\mathcal{S}$. The policy space, and thus its complexity, is user determined. Simple examples include simple decision trees or univariate-based strategies; more can be found in the references above. Recall that $\pi(s', s_0) = \mathbb{E}[Y(s')] - \mathbb{E}[Y(s_0)] = \mathbb{E}[(s'(\boldsymbol{X}) - s_0(\boldsymbol{X}))\tau(\boldsymbol{X})]$, where $\tau(\boldsymbol{x}) = \mathbb{E}[Y(1) - Y(0) \mid \boldsymbol{X} = \boldsymbol{x}]$

is the conditional average treatment effect. Given a space $\mathcal{S}$, we wish to find the policy $s_\star(\boldsymbol{x}) \in \mathcal{S}$ which solves $\max_{s' \in \mathcal{S}} \pi(s', s_0)$. The main result of Athey and Wager (2018) is that replacing π with the doubly-robust $\hat{\pi}$ of Equation (4.2), and minimizing the empirical analogue of regret, one obtains an estimator $\hat{s}(\boldsymbol{x})$ of the optimal policy that obeys the regret bound $\pi(s_\star, s_0) - \pi(\hat{s}, s_0) = O_P(\sqrt{\mathrm{VC}(\mathcal{S})/n})$ (a formal statement would be notationally burdensome). The complexity of the user-chosen policy space enters the bound through its VC dimension. Simple, interpretable policy classes often have bounded or slowly-growing dimension, implying rapid convergence. Beyond the optimal policy itself, the target for inference would be $\pi(\hat{s}, s_0)$ or $\pi(s_\star, s_0)$, which is to say that the parameter of interest is itself learned from the data, in contrast to the above.

3.4   Other Estimands

There are of course many other contexts where first-step deep learning is useful. Only trivial extensions to the above would be required for other causal effects, such as multi-valued treatments (reviewed by Lechner, 2001; Cattaneo, 2010) and others with doubly-robust estimators (Sloczynski and Wooldridge, 2018). Further, under selection on observables, treatment effects, missing data, measurement error, and data combination are equivalent, and thus all our results apply immediately to those contexts. For reviews of these and Assumption 4 more broadly, see Chen, Hong, and Tarozzi (2004); Tsiatis (2006); Heckman and Vytlacil (2007); Imbens and Wooldridge (2009).

Beyond causal effects, any estimand with a locally/doubly robust estimator depending only on conditional expectations can be covered using the results of Section 2. (Estimands requiring density estimation require further study; see Liang (2018) for recent results.) Our results can be used as an ingredient in verifying the conditions of Chernozhukov, Escanciano, Ichimura, Newey, and Robins (2018, Section 7), who treat more general semiparametric estimands using local robustness, sometimes relying on sample splitting or cross fitting. Our results can thus be used in IV models (Belloni, Chen, Chernozhukov, and Hansen, 2012), partial linear models (Belloni, Chernozhukov, and Hansen, 2014), games (Chernozhukov, Escanciano, Ichimura, Newey, and Robins, 2018), differences-in-differences (Sant'Anna and Zhao, 2018), and other areas (Belloni, Chernozhukov, Chetverikov, Hansen, and Kato, 2018). The formal theorems would be very similar to results below, and we defer to these works for precise statements.

More broadly, the learning of features using deep neural networks is becoming increasingly

popular and our results speak to this context directly. To illustrate, consider the simple example of a linear model where some predictors are features learned from independent data. Here, the object of interest is the fixed-dimension coefficient vector $\boldsymbol{\lambda}$, which we assume can be partitioned as $\boldsymbol{\lambda} = (\boldsymbol{\lambda}_1', \boldsymbol{\lambda}_2')'$ according to the model $Y = \boldsymbol{f}(\boldsymbol{X})'\boldsymbol{\lambda}_1 + W'\boldsymbol{\lambda}_2 + \varepsilon$. The features $\boldsymbol{f}(\boldsymbol{X})$, often a "score" of some type, are generally learned from auxiliary (and independent) data. For a recent example, see Liu, Lee, and Srinivasan (2017). In such cases, inference on $\boldsymbol{\lambda}$ can proceed directly, as long as care is taken to interpret the results. See Section 4.2.

4 Asymptotic Inference for Full-Population Averages

We now turn to asymptotic inference for the causal parameters discussed above. We first define the estimators, which are based on sample averages of the (uncentered) influence functions (3.4) and (3.8). We then give generic for single averages which can then be combined for inference on a given parameter of interest. Below we discuss inference under randomized treatment and using sample splitting.

Throughout, we assume we have a sample $\{\boldsymbol{z}_i = (y_i, t_i, \boldsymbol{x}_i')'\}_{i=1}^n$ from $\boldsymbol{Z} = (Y, T, \boldsymbol{X}')'$. We then form

$$\hat{\psi}_t(\boldsymbol{z}_i) = \frac{\mathbb{1}\{t_i = t\}(y_i - \hat{\mu}_t(\boldsymbol{x}_i))}{\hat{\mathbb{P}}[T = t \mid \boldsymbol{X} = \boldsymbol{x}_i]} + \hat{\mu}_t(\boldsymbol{x}_i), \tag{4.1}$$

where $\hat{\mathbb{P}}[T = t \mid \boldsymbol{X} = \boldsymbol{x}_i] = \hat{p}(\boldsymbol{x}_i)$ for $t = 1$ and $1 - \hat{p}(\boldsymbol{x}_i)$ for $t = 0$, and similarly we obtain $\hat{\psi}_{t,t'}(\boldsymbol{z}_i)$.

$$\hat{\psi}_{t,t'}(\boldsymbol{z}_i) = \frac{\hat{\mathbb{P}}[T = t' \mid \boldsymbol{X} = \boldsymbol{x}_i]}{\hat{\mathbb{P}}[T = t']} \frac{\mathbb{1}\{t_i = t\}(y_i - \hat{\mu}_t(\boldsymbol{x}_i))}{\hat{\mathbb{P}}[T = t \mid \boldsymbol{X} = \boldsymbol{x}_i]} + \frac{\mathbb{1}\{t_i = t'\}\hat{\mu}_t(\boldsymbol{x}_i)}{\hat{\mathbb{P}}[T = t']},$$

where $\hat{\mathbb{P}}[T = t']$ is simply the sample frequency $\mathbb{E}_n[\mathbb{1}\{t_i = t'\}]$.

For the first stage estimates appearing in (4.1) we use our results on deep nets, and Theorem 1 in particular. Specifically, the estimated propensity score, $\hat{p}(\boldsymbol{x})$, is the estimate that results from solving (2.3), with the MLP architecture, for the logistic loss (2.2) with T as the outcome. Similarly, for each status $t \in \{0, 1\}$, let $\hat{\mu}_t(\boldsymbol{x})$ be the deep-MLP estimate of $f_*(\boldsymbol{x}) = \mathbb{E}[Y|T = t, \boldsymbol{X} = \boldsymbol{x}]$, solving (2.3) for least squares loss, (2.1), with outcome Y, using only observations with $t_i = t$. In the case of binary outcomes, the latter are replaced by logistic regressions.

We then obtain inference using the following results, essentially taken from Farrell (2015).

Similar results are given by Belloni, Chernozhukov, and Hansen (2014); Belloni, Chernozhukov, Fernández-Val, and Hansen (2017); Belloni, Chernozhukov, Chetverikov, Hansen, and Kato (2018). All of these provide high-level conditions for valid inference, and none verify these for deep nets as we do here.

Theorem 3. *Suppose that $\{\boldsymbol{z}_i = (y_i, t_i, \boldsymbol{x}_i')'\}_{i=1}^n$ are i.i.d. obeying Assumption 4 and the conditions Theorem 1 hold with $\beta > d$. Further assume that, for $t \in \{0,1\}$, $\mathbb{E}[(s(\boldsymbol{X})\psi_t(\boldsymbol{Z}))^2|\boldsymbol{X}]$ is bounded away from zero and $\mathbb{E}[(s(\boldsymbol{X})\psi_t(\boldsymbol{Z}))^{4+\delta}|\boldsymbol{X}]$ is bounded from some $\delta > 0$. Then the deep ReLU network estimators defined above obey the following, for $t \in \{0,1\}$,*

(a) $\mathbb{E}_n[(\hat{p}(\boldsymbol{x}_i) - p(\boldsymbol{x}_i))^2] = o_P(1)$ *and* $\mathbb{E}_n\left[(\hat{\mu}_t(\boldsymbol{x}_i) - \mu_t(\boldsymbol{x}_i))^2\right] = o_P(1)$,

(b) $\mathbb{E}_n[(\hat{\mu}_t(\boldsymbol{x}_i) - \mu_t(\boldsymbol{x}_i))^2]^{1/2}\mathbb{E}_n[(\hat{p}(\boldsymbol{x}_i) - p(\boldsymbol{x}_i))^2]^{1/2} = o_P(n^{-1/2})$, *and*

(c) $\mathbb{E}_n[(\hat{\mu}_t(\boldsymbol{x}_i) - \mu_t(\boldsymbol{x}_i))(1 - \mathbb{1}\{t_i = t\}/\mathbb{P}[T = t|\boldsymbol{X} = \boldsymbol{x}_i])] = o_P(n^{-1/2})$,

and therefore, if $\hat{p}(\boldsymbol{x}_i)$ is bounded inside $(0,1)$, for a given $s(\boldsymbol{x})$ and $t \in \{0,1\}$, we have

$$\sqrt{n}\mathbb{E}_n\left[s(\boldsymbol{x}_i)\hat{\psi}_t(\boldsymbol{z}_i) - s(\boldsymbol{x}_i)\psi_t(\boldsymbol{z}_i)\right] = o_P(1) \quad and \quad \frac{\mathbb{E}_n[(s(\boldsymbol{x}_i)\hat{\psi}_t(\boldsymbol{z}_i))^2]}{\mathbb{E}_n[(s(\boldsymbol{x}_i)\psi_t(\boldsymbol{z}_i))^2]} = o_P(1).$$

Further,

$$\sqrt{n}\mathbb{E}_n\left[\hat{\psi}_{t,t'}(\boldsymbol{z}_i) - \psi_{t,t'}(\boldsymbol{z}_i)\right] = o_P(1) \quad and \quad \frac{\mathbb{E}_n[\hat{\psi}_{t,t'}(\boldsymbol{z}_i)^2]}{\mathbb{E}_n[\psi_{t,t'}(\boldsymbol{z}_i)^2]} = o_P(1).$$

This result, our main inference contribution, shows exactly how deep learning delivers valid asymptotic inference for our parameters of interest. Theorem 1 (a generic result using Theorem 2 could be stated) proves that the nonparametric estimates converge sufficiently fast, as formalized by conditions (a), (b) and (c), enabling feasible semiparametric efficient inference. In general, these are implied by, but may be weaker than, the requirement of that the first step estimates converge faster than $n^{-1/4}$, which our results yield for deep ReLU nets. The first is a mild consistency requirement. The second requires a rate, but on the product of the two estimates, which can be satisfied under weaker conditions. Finally, the third condition is the strongest. Intuitively, this condition arises from a "leave-in" type remainder, and as such, it can be weakened using cross splitting Chernozhukov, Chetverikov, Demirer, Duflo, Hansen, Newey, and Robins (2018); Newey and Robins (2018). We opt to maintain (c) exactly because deep nets are not amenable to either

simple leave-one-out forms (as are, e.g., classical kernel regression) or to sample splitting, being a data hungry method the gain in rate requirements may not be worth the price paid in constants. We use our localization approach to verify (c), see Lemma 11, we may also be of interest in future applications of second-step inference using machine learning methods.

From this result we immediately obtain inference for all the causal parameters discussed above. For the full-population averages, for example, we would form

$$\hat{\tau} = \mathbb{E}_n \left[\hat{\psi}_1(\boldsymbol{z}_i) - \hat{\psi}_0(\boldsymbol{z}_i) \right],$$
$$\hat{\pi}(s) = \mathbb{E}_n \left[s(\boldsymbol{x}_i)\hat{\psi}_1(\boldsymbol{z}_i) + (1 - s(\boldsymbol{x}_i))\hat{\psi}_0(\boldsymbol{z}_i) \right], \tag{4.2}$$
$$\hat{\pi}(s', s_0) = \mathbb{E}_n \left[[s'(\boldsymbol{x}_i) - s_0(\boldsymbol{x}_i)]\hat{\psi}_1(\boldsymbol{z}_i) - [s'(\boldsymbol{x}_i) - s_0(\boldsymbol{x}_i)]\hat{\psi}_0(\boldsymbol{z}_i) \right].$$

The estimator $\hat{\tau}$ is exactly the doubly/locally robust estimator of the average treatment effect that is standard in the literature. The estimators for profits can be thought of as the doubly robust version of the constructs described in Hitsch and Misra (2018). Furthermore, to add a per-unit cost of treatment/targeting c and a margin m, simply replace ψ_1 with $m\psi_1 - c$ and ψ_0 with $m\psi_0$. Similarly, $\hat{\tau}_{1,0}$, $\hat{\Delta}_X$, and $\hat{\Delta}_\mu$ would be linear combinations of different $\hat{\rho}_{t,t'} = \mathbb{E}_n[\hat{\psi}_{t,t'}(\boldsymbol{z}_i)]$.

It is immediate from Theorem 3 that all such estimators are asymptotically Normal. The asymptotic variance can be estimated by simply replacing the sample first moments of (4.2) with second moments. That is, looking at $\hat{\pi}(s)$ to fix ideas,

$$\sqrt{n}\hat{\Sigma}^{-1/2} \left(\hat{\pi}(s) - \pi(s) \right) \xrightarrow{d} \mathcal{N}(0,1), \quad \text{with} \quad \hat{\Sigma} = \mathbb{E}_n \left[\left(s(\boldsymbol{x}_i)\hat{\psi}_1(\boldsymbol{z}_i) + (1 - s(\boldsymbol{x}_i))\hat{\psi}_0(\boldsymbol{z}_i) \right)^2 \right] - \hat{\pi}(s)^2.$$

The others are similar. Furthermore, Theorem 3 can be generalized straightforwardly to provide inference that is uniformly valid over the classes data-generating processes for which our assumptions hold uniformly, following the approach of Romano (2004), exactly as in Belloni, Chernozhukov, and Hansen (2014) or Farrell (2015). It may also be possible to employ recently developed extensions to doubly robust estimation (Tan, 2018) and inverse weighting (Ma and Wang, 2018), which may be beneficial in applications.

4.1 Inference Under Randomization

Our analysis thus far has focused on observational data, but it is worth spelling out results for randomized experiments. This is particularly important in the Internet age, where experimentation is common, vast amounts of data are available, and effects are often small in magnitude (Taddy, Gardner, Chen, and Draper, 2015). Indeed, our empirical illustration, detailed in the next section, stems from an experiment with 300,000 units and hundreds of covariates. When treatment is randomized, inference can be done directly using the mean outcomes in the treatment and control groups, such as the difference for the average treatment effect or the corresponding weighted sum for profit. However, pre-treatment covariates can be used to increase efficiency (Hahn, 2004).

We will focus on the simple situation of a purely randomized binary treatment, but our results can be extended naturally to other randomization schemes. We formalize this with the following.

Assumption 5 (Randomized Treatment). *T is independent of $Y(0)$, $Y(1)$, and X, and is distributed Bernoulli with parameter p^*, such that $\bar{p} \leq p^* \leq 1 - \bar{p}$ for some $\bar{p} > 0$.*

Under this assumption, the obvious simplification is that the propensity score need not be estimated using the covariates, but can be replaced with the (still nonparametric) sample frequency: $\hat{p}(\boldsymbol{x}_i) \equiv \hat{p} = \mathbb{E}_n[t_i]$. This is plugged into Equation (4.2) and estimation and inference proceeds as above. Only rate conditions on the regression functions $\hat{\mu}_t(x)$ are needed. Further, conditions (a) and (b) of Theorem 3 collapse, as $\hat{p}$ is root-n consistent, leaving only condition (c) to be verified. We collect this into the following result, which is a trivial corollary of Theorem 3.

Corollary 3. *Let the conditions of Theorem 3 hold with Assumption 5 in place of Assumption 4. Then deep ReLU network estimators obey*

(a$'$) $\mathbb{E}_n\left[(\hat{\mu}_t(\boldsymbol{x}_i) - \mu_t(\boldsymbol{x}_i))^2\right] = o_P(1)$ *and*

(c$'$) $\mathbb{E}_n[(\hat{\mu}_t(\boldsymbol{x}_i) - \mu_t(\boldsymbol{x}_i))(1 - \mathbb{1}\{t_i = t\}/p^*)] = o_P(n^{-1/2})$

and the conclusions of Theorem 3 hold.

4.2 Sample Splitting

Sample splitting may be used to obtain valid inference in cases, unlike those above, where the parameter of interest itself is learned from the data. For the causal estimands above, the regression

functions and propensity score must be estimated, but these are nuisance functions. This is not true in the inference after policy or feature learning (Sections 3.3 and 3.4). For policy learning, our results can be used to verify the high-level conditions of Athey and Wager (2018), though they require the additional condition of uniform consistency of the first stage estimators, and for machine learning estimators this is not clearly innocuous. However, this gives only estimation of the target parameter.

Sample splitting is used in the obvious way: the first subsample, or more generally, independent auxiliary data, is used to learn the features or optimal policy, and then Theorem 3 or other appropriate result is applied in the second subsample, conditional on the results of the first. For policy learning this delivers valid inference on $\pi(\hat{s})$ or $\pi(\hat{s}, s_0)$, while for the simple example of feature learning in a linear model we obtain inference on the parameters defined by the "model" $Y = \boldsymbol{f}(\boldsymbol{X})'\boldsymbol{\lambda}_1 + W'\boldsymbol{\lambda}_2 + \varepsilon$, where $\boldsymbol{f}(\boldsymbol{X})$ is estimated from auxiliary data. Care must be taken in these case to interpret the results. The results of the first-subsample estimation are effectively conditioned upon in the inference stage, redefining the target parameter to be in terms of the learned object. In many contexts this may be sufficient (Chernozhukov, Demirer, Duflo, and Fernandez-Val, 2018), but further assumptions will generally be needed to assume that the first subsample has recovered the true population object. To fix ideas, consider policy learning: inference on $\pi(\hat{s}, s_0)$, conditional on the learned map $\hat{s}(\boldsymbol{x})$, is immediate and requires no assumptions, but inference on $\pi(s_\star, s_0)$ is not obvious without further conditions.

5   Empirical Application

To illustrate our results, Theorems 1 and 3 in particular, we study, from a marketing point of view, a randomized experiment from a large US retailer of consumer products. The outcome of interest is consumer spending and the treatment is a catalog mailing. The firm sells directly to the customer (as opposed to via retailers) using a variety of channels such as the web and mail. The data consists of nearly three hundred thousand (292,657) consumers chosen at random from the retailer's database. Of these, 2/3 were randomly chosen to receive a catalog, and in addition to treatment status, we observe roughly one hundred fifty covariates, including demographics, past purchase behaviors, interactions with the firm, and other relevant information. For more detail

on this data, as well as a complete discussion of the decision making issues, we refer the reader to Hitsch and Misra (2018) (we use the 2015 sample). That paper studied various estimators, both traditional and modern, of average and heterogeneous causal effects. Importantly, they did not consider neural networks. Our results suggest that deep nets are at least as good as (and sometimes better) that the best methods found by Hitsch and Misra (2018).

In general, a key element of a firm's toolkit is the design and implementation of targeted marketing instruments. These instruments, aiming to induce demand, often contain advertising and informational content about the firms offerings. The targeting aspect thus boils down to the selection of which particular customers should be sent the material. This is a particularly important decision since the costs of creation and dissemination the material can accumulate rapidly, particularly over a large customer base. For a typical retailer engaging in direct marketing the costs of sending out a catalog can be cost close to a dollar per targeted customer. With millions of catalogs being sent out, the cost of a typical campaign is quite high.

Given these expenses an important problem for firms is ascertaining the causal effects of such targeted mailing, and then using these effects to evaluate potential targeting strategies. At a high level, this approach is very similar to modern personalized medicine where treatments have to be targeted. In these contexts, both the treatment and the targeting can be extremely costly, and thus careful assessment of $\pi(s)$ (interpreted as welfare) is crucial for decision making.

The outcome of interest for the firm is customer spending. This is the total amount of money that a given customer spends on purchases of the firm's products, within a specified time window. For the experiment in question the firm used a window of three months, and aggregated sales from all available purchase channels including phone, mail, and the web. In our data 6.2% of customers made a purchase. Overall mean spending is \$7.31; average spending conditional on buying is \$117.7, with a standard deviation of \$132.44. Figure 3 displays the complete density of spending conditional on a purchase, which is quite skewed. The idea then is to examine the incremental effect that the catalog had on this spending metric. Table 1 presents summary statistics for the outcome and treatment.
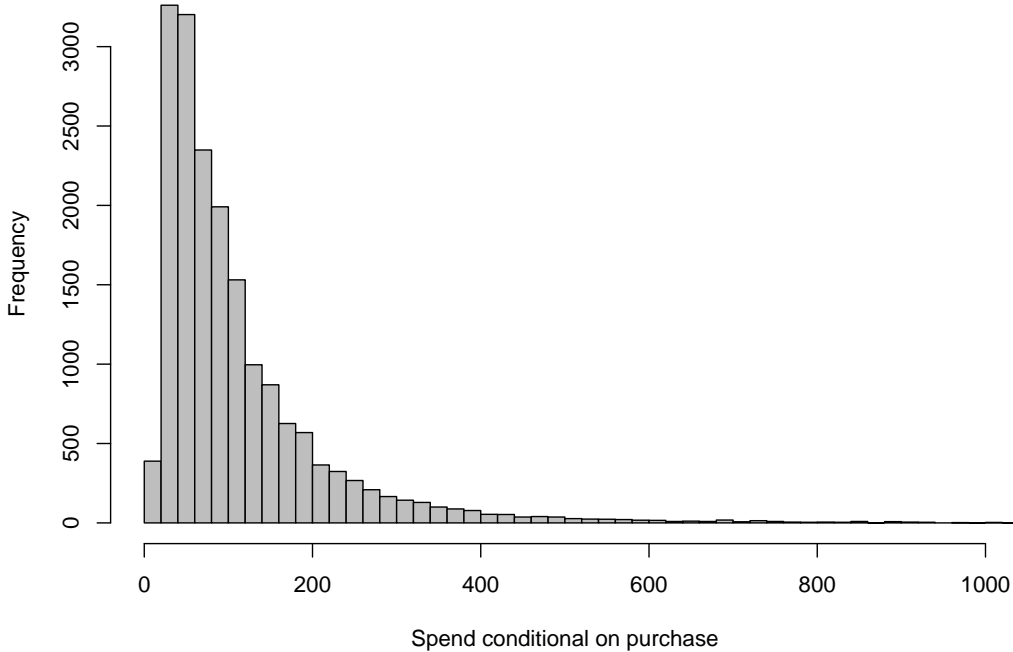
Figure 3: Spend Conditional on Purchase

5.1 Implementation Details

We estimated deep neural nets under a variety of architecture choices. In what follows we present eight examples and focus on one particular architecture to compute various statistics and tests to illustrate the use of the theory developed above. All computation was done using TensorFlow™.

For treatment effect and profit estimation we follow Equations (4.1) and (4.2). Because treatment is randomized, we apply Corollary 3, and thus, only require estimates of the regression functions $\mu_t(\boldsymbol{x}) = E[Y(t)|\boldsymbol{X} = \boldsymbol{x}]$, $t \in \{0, 1\}$. An important implementation detail, from a computation point of view (recall Remark 2) is that we will estimate μ_0 and μ_1 jointly (results from

Table 1: Summary Statistics

	Mean	SD	N
Purchase	0.062	0.24	292657
Spend	7.311	43.55	292657
Spend Conditional on Purchase	117.730	132.44	18174
Treatment	0.669	0.47	292657

separate estimation are available). To be precise, recalling Equations (2.1) and (2.3), we solve

$$
\begin{pmatrix} \hat{\mu}_0(\boldsymbol{x}) \\ \hat{\tau}(\boldsymbol{x}) = \hat{\mu}_1(\boldsymbol{x}) - \hat{\mu}_0(\boldsymbol{x}) \end{pmatrix} := \underset{\tilde{\mu}_0, \tilde{\tau}}{\arg\min} \sum_{i=1}^{n} \frac{1}{2} \Big(y_i - \tilde{\mu}_0(\boldsymbol{x}_i) - \tilde{\tau}(\boldsymbol{x}_i) t_i \Big)^2
$$

where the minimization is over the relevant network architecture. In the context of our empirical example y_i is the costumer's spending, $\boldsymbol{x}_i$ are her characteristics, and t_i indicates receipt of a catalog. In this format, $\mu_0(\boldsymbol{x}_i)$ reflects base spending and $\tau(\boldsymbol{x}) = \mu_1(\boldsymbol{x}_i) - \mu_0(\boldsymbol{x}_i)$ is the conditional average treatment effect of the catalog mailing. In our application, this joint estimation outperforms separately estimating each $\mu_t(\boldsymbol{x})$ on the respective samples (though these two approaches are equivalent theoretically).

The details of the eight deep net architectures are presented in Table 2. See Section 2.1 for an introduction to the terminology and network construction. Most yielded similar results, both in terms of fit and final estimates. A key measure of fit reported in the final column of the table is the portion of $\hat{\tau}(\boldsymbol{x}_i)$ that were negative. As argued by Hitsch and Misra (2018), it is implausible under standard marketing or economic theory that receipt of a catalog causes lower purchasing. On this metric of fit, deep nets perform as well as, and sometimes better than, the best methods found by Hitsch and Misra (2018): Causal KNN with Treatment Effect Projections (detailed therein) or Causal Forests (Wager and Athey, 2018). Figure 4 shows the distribution of $\hat{\tau}(\boldsymbol{x}_i)$ across customers for each of the eight architectures. While there are differences in the shapes of the densities, the mean and variance estimates are nonetheless quite similar.

5.2 Results

We present results for treatment effects, utility/profits, and targeting policy evaluations. Table 3 shows the estimates of the average treatment effect from the eight network architectures along with their respective 95% confidence intervals. These results are constructed following Section 4, using Equations (4.1) and (4.2) in particular, and valid by Corollary 3. All eight specifications yield quite similar results. Furthermore, because this is an experiment, we can compare to the standard unadjusted difference in means, which yields an average treatment effect of 2.632.

Turning to expected profits, we estimate $\pi(s) = \mathbb{E}\big[s(\boldsymbol{X})(mY(1) - c) + (1 - s(\boldsymbol{X}))\, mY(0)\big]$,

Table 2: Deep Network Architectures

Architecture	Learning Rate	Widths $[H_1, H_2, ...]$	Dropout $[H_1, H_2, ...]$	Total Parameters	Validation Loss	Training Loss	$\mathbb{P}_n[\hat{\tau}(\boldsymbol{x}_i) < 0]$
1	0.0003	[60]	[0.5]	8702	1405.62	1748.91	0.0014
2	0.0003	[100]	[0.5]	14502	1406.48	1751.87	0.0251
3	0.0001	[30, 20]	[0.5, 0]	4952	1408.22	1751.20	0.0072
4	0.0009	[30, 10]	[0.3, 0.1]	4622	1408.56	1751.62	0.0138
5	0.0003	[30, 30]	[0, 0]	5282	1403.57	1738.59	0.0226
6	0.0003	[30, 30]	[0.5, 0]	5282	1408.57	1755.28	0.0066
7	0.0003	[100, 30, 20]	[0.5, 0.5, 0]	17992	1408.62	1751.52	0.0103
8	0.00005	[80, 30, 20]	[0.5, 0.5, 0]	14532	1413.70	1756.93	0.0002

Notes: All networks use the ReLU activation function. The width of each layer is shown, e.g. Architecture 3 consists of two layers, with 30 and 20 hidden units respectively. The final column shows the portion of estimated individual treatment effects below zero.

Figure 4: Conditional Average Treatment Effects Across Architectures
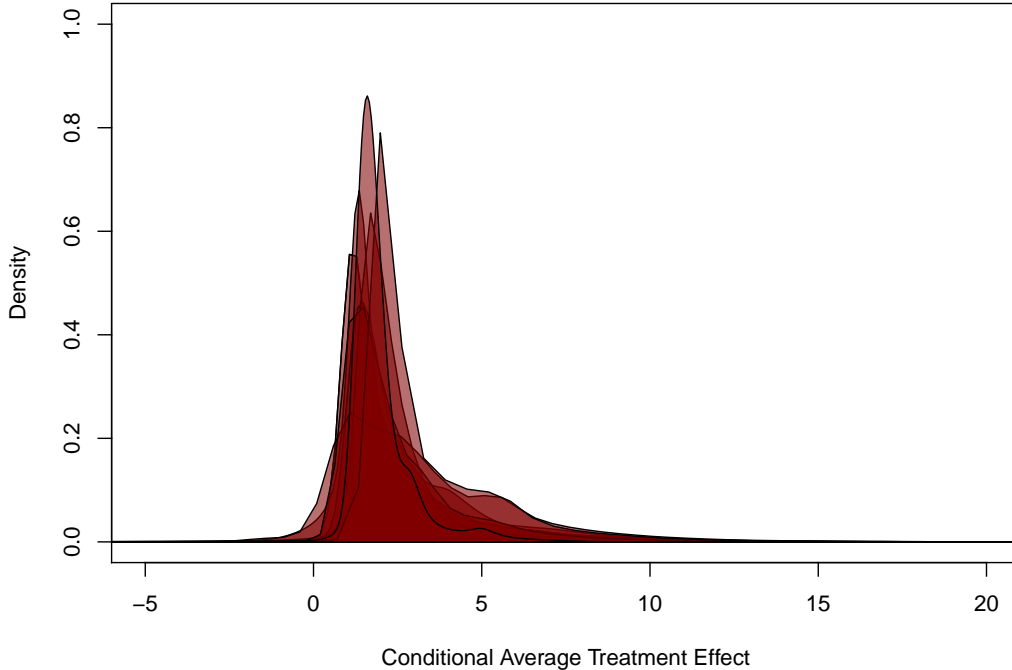
adding a profit margin m and a mailing cost c to (3.2) (our NDA with the firm forbids revealing m and c). We consider three different counterfactual policies $s(\boldsymbol{x})$: (i) *never* treat, $s(\boldsymbol{x}) \equiv 0$; (ii) a *blanket* treatment, $s(\boldsymbol{x}) \equiv 1$; (iii) a *loyalty* policy, $s(\boldsymbol{x}_i) = 1$ only for those who had purchased in

Table 3: Average Treatment Effect Estimates and 95% Confidence Intervals

Architecture	Average Treatment Effect $(\hat{\tau})$	95% Confidence Interval
1	2.606	[2.273 , 2.932]
2	2.577	[2.252 , 2.901]
3	2.547	[2.223 , 2.872]
4	2.488	[2.160 , 2.817]
5	2.459	[2.127 , 2.791]
6	2.430	[2.093 , 2.767]
7	2.400	[2.057 , 2.744]
8	2.371	[2.021 , 2.721]

Table 4: Counterfactual Profits from Three Targeting Strategies

Architecture	Never Treat		Blanket Treatment		Loyalty Policy	
	$\hat{\pi}(s)$	95% CI	$\hat{\pi}(s)$	95% CI	$\hat{\pi}(s)$	95% CI
1	2.016	[1.923 , 2.110]	2.234	[2.162 , 2.306]	2.367	[2.292 , 2.443]
2	2.022	[1.929 , 2.114]	2.229	[2.157 , 2.301]	2.363	[2.288 , 2.438]
3	2.027	[1.934 , 2.120]	2.224	[2.152 , 2.296]	2.358	[2.283 , 2.434]
4	2.037	[1.944 , 2.130]	2.213	[2.140 , 2.286]	2.350	[2.274 , 2.425]
5	2.043	[1.950 , 2.136]	2.208	[2.135 , 2.281]	2.345	[2.269 , 2.422]
6	2.048	[1.954 , 2.142]	2.202	[2.128 , 2.277]	2.341	[2.263 , 2.418]
7	2.053	[1.959 , 2.148]	2.197	[2.122 , 2.272]	2.336	[2.258 , 2.414]
8	2.059	[1.963 , 2.154]	2.192	[2.116 , 2.268]	2.332	[2.253 , 2.411]

the prior calendar year. Results are shown in Table 4. There is close agreement among the eight architectures both numerically and substantially: it is clear that profits from the three policies are ordered as $\pi(\text{never}) < \pi(\text{blanket}) < \pi(\text{loyalty})$.

5.2.1 Optimal Targeting

To explore further, we focus on architecture #3 and study subpopulation treatment targeting strategies following the ideas of Section 3.3. (The other architectures yield similar results, so we omit them.) Architecture #3 has depth $L = 2$ with widths $H_1 = 30$ and $H_2 = 20$. The learning rate was set at 0.0001 and the specification had a total of 4,952 parameters. For this architecture, recalling Remark 1, we added dropout for the second layer with a fixed probability of 1/2. Using this architecture, we compare the blanket strategy (so $s_0(\boldsymbol{x}) = 1$) to targeting customers with spend of at least $\bar{y}$ dollars in the prior calendar year (prior spending is one of the covariates), in $50 increments to $1200. The policy class is therefore $\mathcal{S} = \{s(\boldsymbol{x}) = \mathbb{1}(\texttt{prior spend} >$

Figure 5: Expected Profits from Threshold Targeting Based on Prior Year Spend
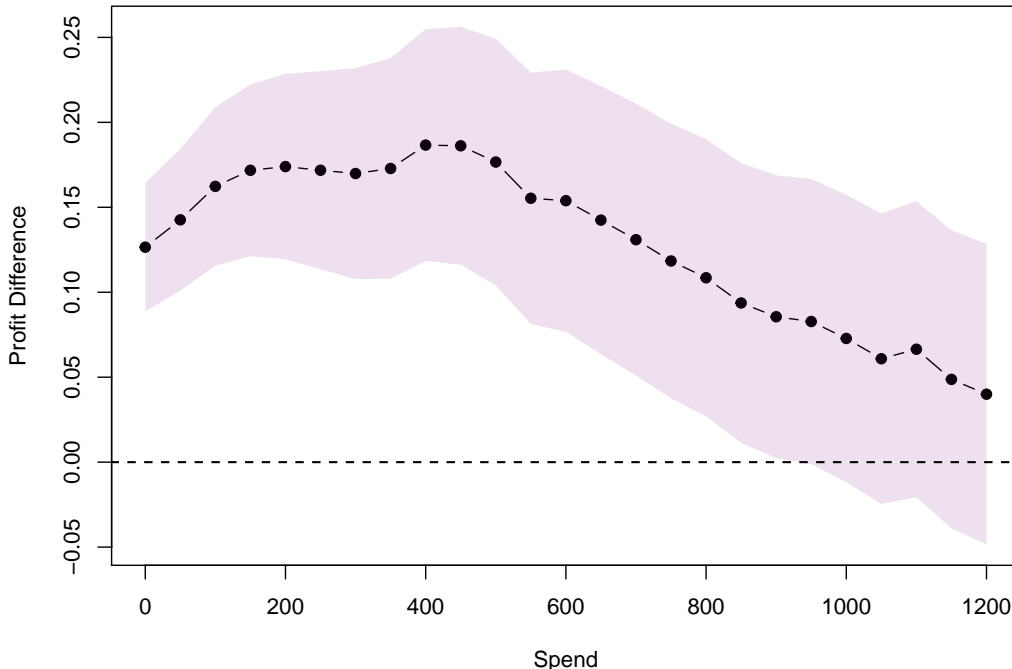
$\bar{y}), \bar{y} = 0, 50, 100, \ldots, 1150, 1200\}$. Figure 5 presents the results. The black dots show the difference $\left\{\pi(\text{spend} > \bar{y}) - \pi(\text{blanket})\right\}$ and the shaded region gives a *pointwise* 95% confidence band (to ease presentation, sample splitting is not used). We see that there is a significant different between various choices of $\bar{y}$. Initially, targeting customers with higher spend yields higher profits, as would be expected, but this effect diminishes beyond a certain $\bar{y}$, roughly \$500, as fewer and fewer are targeted. The optimal policy estimate is $\hat{s}(\boldsymbol{x}) = \mathbb{1}(\texttt{prior spend} > 400)$. In general, simpler policy classes may yield better decisions, but it is certainly possible to expand our search to different $\mathcal{S}$ by considering further covariates and/or transformations.

6   Monte Carlo Analysis

We conducted a set of Monte Carlo experiments to evaluate our theoretical results. We will study inference on the average treatment effect, τ of (3.1), under different data generating processes (DGPs). In each DGP we take $n = 10,000$ i.i.d. samples and use 1,000 replications. For either

$d = 20$ or 100, $\boldsymbol{X}$ includes a constant term and $d - 1$ independent $\mathcal{U}(0, 1)$. Treatment assignment is Bernoulli with probability $p(\boldsymbol{x})$, where $p(\boldsymbol{x})$ is the propensity score. We consider both (i) randomized treatments with $p(\boldsymbol{x}) = 0.5$ and (ii) observational data with $p(\boldsymbol{x}) = (1 + \exp(-\boldsymbol{\alpha}_p' \boldsymbol{x}))^{-1}$, where $\alpha_{p,1} = 0.09$ and the remainder are drawn as $\mathcal{U}(-0.55, 0.55)$, and then fixed for the simulations. For $d = 100$, we maintain $\|\boldsymbol{\alpha}_p\|_0 = 20$ for the simplicity. These generate propensities with an interquartile range of approximately $(0.30, .0.75)$ and mean roughly 0.52.

Given covariates and treatment assignment, the outcomes are generated according

$$y_i = \mu_0(\boldsymbol{x}_i) + \tau(\boldsymbol{x}_i) t_i + \varepsilon_i, \qquad \mu_0(\boldsymbol{x}) = \boldsymbol{\alpha}_\mu' \boldsymbol{x} + \boldsymbol{\beta}_\mu' \varphi(\boldsymbol{x}), \qquad \tau(x_i) = \boldsymbol{\alpha}_\tau' \boldsymbol{x} + \boldsymbol{\beta}_\tau' \varphi(\boldsymbol{x}),$$

where $\varepsilon_i \sim \mathcal{N}(0, 1)$ and $\varphi(\boldsymbol{x})$ are second-degree polynomials including pairwise interactions. For $\mu_0(\boldsymbol{x})$ and $\tau(\boldsymbol{x})$ we consider two cases, linear and nonlinear models. In both cases the intercepts are $\alpha_{\mu,1} = 0.09$ and $\alpha_{\tau,1} = -0.05$ and slopes are drawn (once) as $\alpha_{\mu,k} \sim \mathcal{N}(0.3, 0.49)$ and $\alpha_{\tau,k} \sim \mathcal{U}(0.1, 0.22)$, $k = 2, \ldots, d$. The linear models set $\boldsymbol{\beta}_\mu = \boldsymbol{\beta}_\tau = \boldsymbol{0}$ while the nonlinear models take $\beta_{\mu,k} \sim \mathcal{N}(0.01, 0.09)$ and $\beta_{\tau,k} \sim \mathcal{U}(-0.05, 0.06)$. Altogether, this yields eight designs: $d = 20$ or 100, $p(\boldsymbol{x})$ constant or not, and outcome models linear or nonlinear.

We consider two different network architectures for estimation. Both are ReLU-based MLPs, but the first has three layers, with widths 60, 30, and 20, while the second has five layers, with widths 20,15,15,10,10, and 5. Table 5 shows the results for all eight DGPs: panel (a) shows randomized treatment while panel (b) shows results mimicking observational data. Overall, the results reported show excellent performance of deep learning based semiparametric inference. The bias is minimal and the coverage is quite accurate, while the interval length is under control. Notice that the two architectures yield similar results, neither dominates the other, but that the more complex architecture does not suffer from length inflation.

Neither architecture used regularization. In our empirical application, most architectures employed dropout, a common method of regularization; see Remark 1. However, results without dropout were no worse (see Architecture 5 in Tables 3 and 4). As is typical, regularization can introduce bias problems. To explore this, we added regularization to architecture 1 and reran the simulations. The corresponding results are shown in Table 6. In some, not all, cases the coverage remains accurate, but with greatly increased bias and interval length compared to Table 5. The

Table 5: Simulation Results

(a) Constant Propensity Score

Model	Architecture	20 Covariates			100 Covariates		
		Bias	IL	Coverage	Bias	IL	Coverage
Linear	1	-0.00001	0.079	0.946	-0.00029	0.080	0.940
	2	0.00065	0.079	0.942	0.00024	0.081	0.949
Nonlinear	1	0.00027	0.079	0.945	0.00125	0.147	0.912
	2	-0.00025	0.081	0.939	0.00030	0.164	0.959

(b) Nonconstant Propensity Score

Model	Architecture	20 Covariates			100 Covariates		
		Bias	IL	Coverage	Bias	IL	Coverage
	1	-0.00027	0.080	0.942	0.00025	0.081	0.928
Linear	2	-0.00100	0.079	0.960	-0.00080	0.081	0.949
	1	-0.00116	0.080	0.950	-0.00117	0.159	0.949
Nonlinear	2	-0.00155	0.081	0.953	-0.00015	0.165	0.856

Table 6: Adding Dropout to Architecture 1

Outcome Model	Propensity Score	20 Covariates			100 Covariates		
		Bias	IL	Coverage	Bias	IL	Coverage
Linear	*Constant*	0.0004	0.098	0.955	-0.0005	0.199	0.978
		0.0018	0.133	0.979	-0.0019	0.420	0.974
Linear	*Constant*	-0.0098	0.099	0.942	0.0008	0.191	0.964
		-0.0087	0.123	0.748	-0.0599	0.445	0.960

results preach caution when applying regularization in applications.

7   Conclusion

The utility of deep learning in social science applications is still a subject of interest and debate. While there is an acknowledgment of its predictive power, there has been limited adoption of deep learning in social sciences such as Economics. Some part of the reluctance to adopting these methods stems from the lack of theory facilitating use and interpretation. We have shown, both theoretically as well as empirically, that these methods can offer excellent performance.

In this paper, we have given a formal proof that inference can be valid after using deep learning methods for first-step estimation. To the best of our knowledge, ours is the first inference result using deep nets. Our results thus contribute directly to the recent explosion in both theoretical

and applied research using machine learning methods in economics, and to the recent adoption of deep learning in empirical settings. We obtained novel bounds for deep neural networks, speaking directly to the modern (and empirically successful) practice of using fully-connected feedfoward networks. Our results allow for different network architectures, including fixed width, very deep networks. To obtain these rates we have used a novel proof strategy, departing from past analyses of neural networks in the sieve estimation literature. Our results cover nonparametric conditional expectations, and we gave concrete rates for least squares and logistic loss, thus covering most nonparametric practice. We used our bounds to deliver fast convergence rates allowing for second-stage inference on a finite-dimensional parameter of interest.

There are practical implications of the theory presented in this paper. We focused on semiparametric causal effects as a concrete illustration, but deep learning is a potentially valuable tool in many diverse economic settings. Our results allow researchers to embed deep learning into standard econometric models such as linear regressions, generalized linear models, and other forms of limited dependent variables models (e.g. censored regression). These results can also be used as a starting point for constructing deep learning implementations of two-step estimators in the context of selection models, dynamic discrete choice, and the estimation of games.

To be clear, we see our paper as a first step in the exploration of deep learning as a tool for economic applications. There are a number of opportunities, questions, and challenges that remain. For example, factor models in finance might benefit from the use of auto-encoders and recurrent neural nets may have applications in time series. For some estimands, it may be crucial to estimate the density as well, and this problem can be challenging in high dimensions. Deep nets, in the form of Generative Adversarial Networks are a promising tool for density estimation. There are also interesting questions remaining as to an optimal network architecture, and if this can be itself learned from the data, as well as computational and optimization guidance. Research into these further applications and structures is underway.

8 References

ABADIE, A., AND M. D. CATTANEO (2018): "Econometric Methods for Program Evaluation," *Annual Review of Economics*, 10, 465–503.

ANTHONY, M., AND P. L. BARTLETT (1999): *Neural Network Learning: Theoretical Foundations*. Campbridge University Press.

ATHEY, S., G. IMBENS, T. PHAM, AND S. WAGER (2017): "Estimating average treatment effects: Supplementary analyses and remaining challenges," *American Economic Review: Papers & Proceeding*, 107(5), 278–81.

ATHEY, S., G. W. IMBENS, AND S. WAGER (2018): "Approximate residual balancing: debiased inference of average treatment effects in high dimensions," *Journal of the Royal Statistical Society, Series B*, 80(4), 597–623.

ATHEY, S., AND S. WAGER (2018): "Efficient Policy Learning," *arXiv preprint arXiv:1702.02896*.

BARRON, A. R. (1993): "Universal approximation bounds for superpositions of a sigmoidal function," *IEEE Transactions on Information theory*, 39(3), 930–945.

BARTLETT, P. L., O. BOUSQUET, S. MENDELSON, ET AL. (2005): "Local rademacher complexities," *The Annals of Statistics*, 33(4), 1497–1537.

BARTLETT, P. L., N. HARVEY, C. LIAW, AND A. MEHRABIAN (2017): "Nearly-tight VC-dimension bounds for piecewise linear neural networks," in *Proceedings of the 22nd Annual Conference on Learning Theory (COLT 2017)*.

BAUER, B., AND M. KOHLER (2017): "On Deep Learning as a remedy for the curse of dimensionality in nonparametric regression," Discussion paper, Technical report.

BELLONI, A., D. CHEN, V. CHERNOZHUKOV, AND C. HANSEN (2012): "Sparse models and methods for optimal instruments with an application to eminent domain," *Econometrica*, 80(6), 2369–2429.

BELLONI, A., V. CHERNOZHUKOV, D. CHETVERIKOV, C. HANSEN, AND K. KATO (2018): "High-Dimensional Econometrics and Generalized GMM," *arXiv preprint arXiv:1806.01888*.

BELLONI, A., V. CHERNOZHUKOV, I. FERNÁNDEZ-VAL, AND C. HANSEN (2017): "Program Evaluation and Causal Inference With High-Dimensional Data," *Econometrica*, 85(1), 233–298.

BELLONI, A., V. CHERNOZHUKOV, AND C. HANSEN (2014): "Inference on Treatment Effects after Selection Amongst High-Dimensional Controls," *Review of Economic Studies*, 81, 608–650.

BELLONI, A., V. CHERNOZHUKOV, AND L. WANG (2011): "Square-root lasso: pivotal recovery of sparse signals via conic programming," *Biometrika*, 98(4), 791–806.

BICKEL, P. J., Y. RITOV, AND A. B. TSYBAKOV (2009): "Simultaneous Analysis of LASSO and Dantzig Selector," *The Annals of Statistics*, 37(4), 1705–1732.

BLINDER, A. (1973): "Wage Discrimination: Reduced Form and Structural Estimates," *Journal of Human Resources*, 8(4), 436–455.

CATTANEO, M. D. (2010): "Efficient Semiparametric Estimation of Multi-valued Treatment Effects under Ignorability," *Journal of Econometrics*, 155(2), 138–154.

CATTANEO, M. D., M. JANSSON, AND X. MA (2018): "Two-step Estimation and Inference with Possibly Many Included Covariates," *arXiv:1807.10100, Review of Economic Studies*, forthcoming.

CHEN, X. (2007): "Large Sample Sieve Estimation of Semi-Nonparametric Models," in *Handbook of Econometrics*, ed. by J. Heckman, and E. Leamer, vol. 6B of *Handbook of Econometrics*, chap. 76. Elsevier.

CHEN, X., H. HONG, AND A. TAROZZI (2004): "Semiparametric Efficiency in GMM Models of Nonclassical Measurament Errors, Missing Data and Treatment Effects," *Cowles Foundation Discussion Paper No. 1644*.

CHEN, X., AND X. SHEN (1998): "Sieve extremum estimates for weakly dependent data," *Econometrica*, 66(2), 289–314.

CHEN, X., AND H. WHITE (1999): "Improved rates and asymptotic normality for nonparametric neural network estimators," *IEEE Transactions on Information Theory*, 45(2), 682–691.

CHERNOZHUKOV, V., D. CHETVERIKOV, M. DEMIRER, E. DUFLO, C. HANSEN, W. NEWEY, AND J. ROBINS (2018): "Double/debiased machine learning for treatment and structural parameters," *The Econometrics Journal*, 21(1), C1–C68.

CHERNOZHUKOV, V., M. DEMIRER, E. DUFLO, AND I. FERNANDEZ-VAL (2018): "Generic Machine Learning Inference on Heterogenous Treatment Effects in Randomized Experiments," *arXiv preprint arXiv:1712.04802*.

CHERNOZHUKOV, V., J. C. ESCANCIANO, H. ICHIMURA, W. K. NEWEY, AND J. M. ROBINS (2018): "Locally Robust Semiparametric Estimation," *arXiv:1608.00033*.

DANIELY, A. (2017): "Depth separation for neural networks," *arXiv preprint arXiv:1702.08489*.

FARRELL, M. H. (2015): "Robust Inference on Average Treatment Effects with Possibly More Covariates than Observations," *arXiv:1309.4686, Journal of Econometrics*, 189, 1–23.

FORTIN, N., T. LEMIEUX, AND S. FIRPO (2011): "Decomposition Methods in Economics," vol. 4 of *Handbook of Labor Economics*, pp. 1–102.

GOODFELLOW, I., Y. BENGIO, AND A. COURVILLE (2016): *Deep learning*. MIT Press, Cambridge.

HAHN, J. (1998): "On the Role of the Propensity Score in Efficient Semiparametric Estimation of Average Treatment Effects," *Econometrica*, 66(2), 315–331.

——— (2004): "Functional restriction and efficiency in causal inference," *Review of Economics and Statistics*, 84(1), 73–76.

HANIN, B. (2017): "Universal function approximation by deep neural nets with bounded width and relu activations," *arXiv preprint arXiv:1708.02691*.

HANSEN, C., D. KOZBUR, AND S. MISRA (2017): "Targeted Undersmoothing," *arXiv:1706.07328*.

HARTFORD, J., G. LEWIS, K. LEYTON-BROWN, AND M. TADDY (2017): "Deep iv: A flexible approach for counterfactual prediction," in *International Conference on Machine Learning*, pp. 1414–1423.

HASTIE, T., R. TIBSHIRANI, AND J. FRIEDMAN (2009): *The elements of statistical learning*, Springer Series in Statistics. Springer-Verlag, New York.

HE, K., X. ZHANG, S. REN, AND J. SUN (2016): "Identity mappings in deep residual networks," in *European conference on computer vision*, pp. 630–645. Springer.

HECKMAN, J., AND E. J. VYTLACIL (2007): "Econometric Evaluation of Social Programs, Part I," in *Handbook of Econometrics, vol. VIB*, ed. by J. Heckman, and E. Leamer, pp. 4780–4874. Elsevier Science B.V.

HIRANO, K., AND J. PORTER (2009): "Asymptotics for statistical treatment rules," *Econometrica*, 77(5), 1683–1701.

HITSCH, G. J., AND S. MISRA (2018): "Heterogeneous Treatment Effects and Optimal Targeting Policy Evaluation," *SSRN preprint 3111957*.

HORNIK, K., M. STINCHCOMBE, AND H. WHITE (1989): "Multilayer feedforward networks are universal approximators," *Neural networks*, 2(5), 359–366.

IMBENS, G. W., AND D. B. RUBIN (2015): *Causal Inference in Statistics, Social, and Biomedical Sciences*. Cambridge University Press.

IMBENS, G. W., AND J. M. WOOLDRIDGE (2009): "Recent Developments in the Econometrics of Program Evaluation," *Journal of Economic Literature*, 47(1), 5–86.

JAVANMARD, A., AND A. MONTANARI (2014): "Confidence intervals and hypothesis testing for high-dimensional regression," *The Journal of Machine Learning Research*, 15(1), 2869–2909.

JOHANSSON, F., U. SHALIT, AND D. SONTAG (2016): "Learning representations for counterfactual inference," in *International Conference on Machine Learning*, pp. 3020–3029.

KINGMA, D. P., AND J. BA (2014): "Adam: A method for stochastic optimization," *arXiv preprint arXiv:1412.6980*.

KITAGAWA, E. M. (1955): "Components of a Difference Between Two Rates," *Journal of the American Statistical Association*, 50(272), 1168–1194.

KITAGAWA, T., AND A. TETENOV (2018): "Who should be treated? empirical welfare maximization methods for treatment choice," *Econometrica*, 86(2), 591–616.

KOLTCHINSKII, V. (2006): "Local Rademacher complexities and oracle inequalities in risk minimization," *The Annals of Statistics*, 34(6), 2593–2656.

KOLTCHINSKII, V., AND D. PANCHENKO (2000): "Rademacher processes and bounding the risk of function learning," in *High dimensional probability II*, pp. 443–457. Springer.

KRIZHEVSKY, A., I. SUTSKEVER, AND G. E. HINTON (2012): "Imagenet classification with deep convolutional neural networks," in *Advances in neural information processing systems*, pp. 1097–1105.

LECHNER, M. (2001): "Identification and estimation of causal effects of multiple treatments under the conditional independence assumption," in *Econometric Evaluations of Active Labor Market Policies*, ed. by M. Lechner, and E. Pfeiffer, pp. 43–58. Physica, Heidelberg.

LECUN, Y., L. BOTTOU, Y. BENGIO, AND P. HAFFNER (1998): "Gradient-based learning applied to document recognition," *Proceedings of the IEEE*, 86(11), 2278–2324.

LIANG, T. (2018): "On How Well Generative Adversarial Networks Learn Densities: Nonparametric and Parametric Results," *arXiv:1811.03179*.

LIANG, T., A. RAKHLIN, AND K. SRIDHARAN (2015): "Learning with square loss: Localization through offset Rademacher complexity," in *Conference on Learning Theory*, pp. 1260–1285.

LIU, X., D. LEE, AND K. SRINIVASAN (2017): "Large scale cross category analysis of consumer review content on sales conversion leveraging deep learning," *working paper, NYU Stern*.

MA, X., AND J. WANG (2018): "Robust Inference Using Inverse Probability Weighting," *arXiv preprint arXiv:1810.11397*.

MAKOVOZ, Y. (1996): "Random approximants and neural networks," *Journal of Approximation Theory*, 85(1), 98–109.

MANSKI, C. F. (2004): "Statistical treatment rules for heterogeneous populations," *Econometrica*, 72(4), 1221–1246.

MENDELSON, S. (2003): "A few notes on statistical learning theory," in *Advanced lectures on machine learning*, pp. 1–40. Springer.

MHASKAR, H., AND T. POGGIO (2016a): "Deep vs. shallow networks: An approximation theory perspective," *arXiv preprint arXiv:1608.03287*.

MHASKAR, H. N., AND T. POGGIO (2016b): "Deep vs. shallow networks: An approximation theory perspective," *Analysis and Applications*, 14(06), 829–848.

NAIR, V., AND G. E. HINTON (2010): "Rectified linear units improve restricted boltzmann machines," in *Proceedings of the 27th international conference on machine learning (ICML-10)*, pp. 807–814.

NEWEY, W. K., AND J. M. ROBINS (2018): "Cross-fitting and fast remainder rates for semiparametric estimation," *arXiv preprint arXiv:1801.09138*.

OAXACA, R. (1973): "Male-Female Wage Differentials in Urban Labor Markets," *International Economic Review*, 14(3), 693–709.

PISIER, G. (1981): "Remarques sur un résultat non publié de B. Maurey," in *Séminaire Analyse fonctionnelle (dit Maurey-Schwartz)*, pp. 1–12.

POLSON, N., AND V. ROCKOVA (2018): "Posterior Concentration for Sparse Deep Learning," *arXiv preprint arXiv:1803.09138*.

RAGHU, M., B. POOLE, J. KLEINBERG, S. GANGULI, AND J. SOHL-DICKSTEIN (2017): "On the Expressive Power of Deep Neural Networks," in *Proceedings of the 34th International Conference on Machine Learning*, ed. by D. Precup, and Y. W. Teh, vol. 70 of *Proceedings of Machine Learning Research*, pp. 2847–2854, International Convention Centre, Sydney, Australia. PMLR.

ROBINS, J., L. LI, R. MUKHERJEE, E. TCHETGEN, AND A. VAN DER VAART (2017): "Minimax Estimation of a Functional on a Structured High-Dimensional Model," *The Annals of Statistics*, 45(5), 1951–1987.

ROBINS, J., L. LI, E. TCHETGEN, AND A. VAN DER VAART (2008): "Higher order influence functions and minimax estimation of nonlinear functionals," in *Probability and Statistics: Essays in Honor of David A. Freedman*, ed. by D. Nolan, and T. Speed, vol. 2. Beachwood, Ohio, USA: Institute of Mathematical Statistics.

ROBINS, J. M., A. ROTNITZKY, AND L. ZHAO (1994): "Estimation of Regression Coefficients When Some Regressors Are Not Always Observed," *Journal of the American Statistical Association*, 89(427), 846–866.

——— (1995): "Analysis of Semiparametric Regression Models for Repeated Outcomes in the Presence of Missing Data," *Journal of the American Statistical Association*, 90(429), 846–866.

ROMANO, J. P. (2004): "On non-parametric testing, the uniform behaviour of the *t*-test, and related problems," *Scandinavian Journal of Statistics*, 31(4), 567–584.

SAFRAN, I., AND O. SHAMIR (2016): "Depth separation in relu networks for approximating smooth non-linear functions," *arXiv preprint arXiv:1610.09887*.

SANT'ANNA, P. H. C., AND J. B. ZHAO (2018): "Doubly Robust Difference-in-Differences Estimators," *arXiv:1812.01723*.

SCHMIDT-HIEBER, J. (2017): "Nonparametric regression using deep neural networks with ReLU activation function," *arXiv preprint arXiv:1708.06633*.

SHALIT, U., F. D. JOHANSSON, AND D. SONTAG (2017): "Estimating individual treatment effect: generalization bounds and algorithms," *arXiv preprint arXiv:1606.03976*.

SLOCZYNSKI, T., AND J. M. WOOLDRIDGE (2018): "A General Double Robustness Result for Estimating Average Treatment Effects," *Econometric Theory*, 34(1), 112133.

STONE, C. J. (1982): "Optimal global rates of convergence for nonparametric regression," *The annals of statistics*, pp. 1040–1053.

TADDY, M., M. GARDNER, L. CHEN, AND D. DRAPER (2015): "A nonparametric Bayesian analysis of heterogeneous treatment effects in digital experimentation," *Arxiv preprint arXiv:1412.8563*.

TAN, Z. (2018): "Model-assisted inference for treatment effects using regularized calibrated estimation with high-dimensional data," *arXiv preprint arXiv:1801.09817*.

TELGARSKY, M. (2016): "Benefits of depth in neural networks," *arXiv preprint arXiv:1602.04485*.

TSIATIS, A. A. (2006): *Semiparametric Theory and Missing Data*. Springer, New York.

VAN DE GEER, S., P. BUHLMANN, Y. RITOV, AND R. DEZEURE (2014): "On Asymptotically Optimal Confidence Regions and Tests for High-Dimensional Models," *The Annals of Statistics*, 42(3), 1166–1202.

VAN DER LAAN, M., AND S. ROSE (2001): *Targeted Learning: Causal Inference for Observational and Experimental Data*. Springer-Verlag.

WAGER, S., AND S. ATHEY (2018): "Estimation and Inference of Heterogeneous Treatment Effects using Random Forests," *Journal of the American Statistical Association,* forthcoming.

WESTREICH, D., J. LESSLER, AND M. J. FUNK (2010): "Propensity score estimation: neural networks, support vector machines, decision trees (CART), and meta-classifiers as alternatives to logistic regression," *Journal of clinical epidemiology*, 63(8), 826–833.

WHITE, H. (1989): "Learning in artificial neural networks: A statistical perspective," *Neural computation*, 1(4), 425–464.

――― (1992): *Artificial neural networks: approximation and learning theory*. Blackwell Publishers, Inc.

YAROTSKY, D. (2017): "Error bounds for approximations with deep ReLU networks," *Neural Networks*, 94, 103–114.

――― (2018): "Optimal approximation of continuous functions by very deep ReLU networks," *arXiv preprint arXiv:1802.03620*.

ZHANG, C., S. BENGIO, M. HARDT, B. RECHT, AND O. VINYALS (2016): "Understanding deep learning requires rethinking generalization," *arXiv preprint arXiv:1611.03530*.

A   Proof of Theorems 1 and 2

In this section we provide a proof of Theorems 1 and 2, our main theoretical results for deep ReLU networks. The proof proceeds in several steps. We first give the main breakdown and bound the bias (approximation error) term. We then turn our attention to the empirical process term, to which we apply our localization. Much of the proof uses a generic architecture, and thus pertains to both results. We will specialize the architecture to the multi-layer perceptron only when needed later on. Other special cases and related results are covered in Section B. Supporting Lemmas are stated in Section C.

For notational simplicity we will denote $\widehat{f}_{\text{DNN}} := \hat{f}$, see (2.3), and $\epsilon_{\text{DNN}} := \epsilon_n$, see Assumption 3. As we are simultaneously consider Theorems 1 and 2, the generic notation DNN will be used throughout.

A.1   Main Decomposition and Bias Term

Referring to Assumption 3, define the best approximation realized by the deep ReLU network class $\mathcal{F}_{\text{DNN}}$ as

$$f_n := \underset{\substack{f \in \mathcal{F}_{\text{DNN}} \\ \|f\|_\infty \leq 2M}}{\arg\min} \|f - f_*\|_\infty.$$

By definition, $\epsilon_n := \epsilon_{\text{DNN}} := \|f_n - f_*\|_\infty$.

Recalling the optimality of the estimator in (2.3), we know, as both f_n and $\hat{f}$ are in $\mathcal{F}_{\text{DNN}}$, that

$$-\mathbb{E}_n[\ell(\hat{f}, \boldsymbol{z})] + \mathbb{E}_n[\ell(f_n, \boldsymbol{z})] \geq 0.$$

This result does not hold for f_* in place of f_n, because $f_* \notin \mathcal{F}_{\mathrm{DNN}}$. Using the above display and Lemma 9 (which does not hold with f_n in place of f_* therein), we obtain

$$
\begin{aligned}
c_2\|\hat{f} - f_*\|^2_{L_2(X)} &\leq \mathbb{E}[\ell(\hat{f}, \boldsymbol{z})] - \mathbb{E}[\ell(f_*, \boldsymbol{z})] \\
&\leq \mathbb{E}[\ell(\hat{f}, \boldsymbol{z})] - \mathbb{E}[\ell(f_*, \boldsymbol{z})] - \mathbb{E}_n[\ell(\hat{f}, \boldsymbol{z})] + \mathbb{E}_n[\ell(f_n, \boldsymbol{z})] \\
&= \mathbb{E}\left[\ell(\hat{f}, \boldsymbol{z}) - \ell(f_*, \boldsymbol{z})\right] - \mathbb{E}_n\left[\ell(\hat{f}, \boldsymbol{z}) - \ell(f_*, \boldsymbol{z})\right] + \mathbb{E}_n\left[\ell(f_n, \boldsymbol{z}) - \ell(f_*, \boldsymbol{z})\right] \\
&= (\mathbb{E} - \mathbb{E}_n)\left[\ell(\hat{f}, \boldsymbol{z}) - \ell(f_*, \boldsymbol{z})\right] + \mathbb{E}_n\left[\ell(f_n, \boldsymbol{z}) - \ell(f_*, \boldsymbol{z})\right]. \quad\quad\text{(A.1)}
\end{aligned}
$$

Equation (A.1) is the main decomposition that begins the proof. The decomposition must be done this way because of the above notes regarding f_* and f_n. The first term is the empirical process term that will be treated in the subsequent subsection. For the second term in (A.1), the bias term or approximation error, we apply Bernstein's inequality to find that, with probability at least $1 - e^{-\gamma}$,

$$
\begin{aligned}
\mathbb{E}_n\left[\ell(f_n, \boldsymbol{z}) - \ell(f_*, \boldsymbol{z})\right] &\leq \mathbb{E}\left[\ell(f_n, \boldsymbol{z}) - \ell(f_*, \boldsymbol{z})\right] + \sqrt{\frac{2C_\ell^2\|f_n - f_*\|^2_\infty \gamma}{n}} + \frac{14C_\ell M\gamma}{3n} \\
&\leq \frac{1}{c_2}\mathbb{E}\left[\|f_n - f_*\|^2\right] + \sqrt{\frac{2C_\ell^2\|f_n - f_*\|^2_\infty \gamma}{n}} + \frac{14C_\ell M\gamma}{3n} \\
&\leq \frac{1}{c_2}\epsilon_n^2 + \epsilon_n\sqrt{\frac{2C_\ell^2\gamma}{n}} + \frac{14C_\ell M\gamma}{3n}, \quad\quad\text{(A.2)}
\end{aligned}
$$

using Lemma 9 (wherein c_2 is given) and $\mathbb{E}\left[\|f_n - f_*\|^2\right] \leq \|f_n - f_*\|^2_\infty$, along with the definition of ϵ_n^2, and Lemma 10.

Once the empirical process term is controlled (in Section A.2), the two bounds will be brought back together to compute the final result, see Section A.3.

A.2 Localized Analysis

We now turn to bounding the first term in (A.1) (the empirical processes term) using a novel localized analysis that derives bounds based on scale insensitive complexity measure. The ideas of our localization are rooted in Koltchinskii and Panchenko (2000) and Bartlett, Bousquet, Mendelson, et al. (2005). This proof section proceeds in several steps.

A key quantity is the Rademacher complexity of the function class at hand. Given i.i.d. Rademacher draws, $\eta_i = \pm 1$ with equal probability independent of the data, the random variable $R_n\mathcal{F}$, for a function class $\mathcal{F}$, is defined as

$$
R_n\mathcal{F} := \sup_{f \in \mathcal{F}} \frac{1}{n}\sum_{i=1}^n \eta_i f(x_i).
$$

Intuitively, $R_n\mathcal{F}$ measures how flexible the function class is for predicting random signs. Taking

the expectation of $R_n\mathcal{F}$ conditioned on the data we obtain the *empirical Rademacher complexity*, denoted $\mathbb{E}_\eta[R_n\mathcal{F}]$. When the expectation is taken over both the data and the draws η_i, $\mathbb{E}R_n\mathcal{F}$, we get the *Rademacher complexity*.

A.2.1   Step I: Quadratic Process

The first step is to show that the empirical L_2 norm of $(f-f_*)$ is at most twice the population bound, for certain functions f outside a certain critical radius. This fact will be used later on. Denote $\|f\|_n := \left(\frac{1}{n}\sum_{i=1}^n f(x_i)^2\right)^{1/2}$ to be the empirical L_2-distance. To do so, we study the quadratic process

$$\|f-f_*\|_n^2 - \|f-f_*\|_{L_2(X)}^2 = \mathbb{E}_n(f-f_*)^2 - \mathbb{E}(f-f_*)^2.$$

We will apply the symmetrization of Lemma 6 to $g = (f-f_*)^2$ restricted to a radius $\|f-f_*\|_{L_2(X)} \leq r$. This function g has variance bounded as

$$\mathbb{V}[g] \leq \mathbb{E}[g^2] \leq \mathbb{E}((f-f_*)^4) \leq 4M^2r^2.$$

Writing $g = (f+f_*)(f-f_*)$, we see that by Assumption 1, $|g| \leq 2M|f-f_*| \leq 4M^2$, where the first inequality verifies that g has a Lipschitz constant of $2M$, and second that g itself is bounded. We therefore apply Lemma 6, to obtain, with probability at least $1 - \exp(-\gamma)$, that for any $f \in \mathcal{F}$ with $\|f-f_*\|_{L_2(X)} \leq r$,

$$\mathbb{E}_n(f-f_*)^2 - \mathbb{E}(f-f_*)^2$$
$$\leq 3\mathbb{E}R_n\{g = (f-f_*)^2 : f \in \mathcal{F}, \|f-f_*\|_{L_2(X)} \leq r\} + 2Mr\sqrt{\frac{2\gamma}{n}} + \frac{16M^2}{3}\frac{\gamma}{n}$$
$$\leq 6M\mathbb{E}R_n\{f-f_* : f \in \mathcal{F}, \|f-f_*\|_{L_2(X)} \leq r\} + 2Mr\sqrt{\frac{2\gamma}{n}} + \frac{16M^2}{3}\frac{\gamma}{n}, \qquad (A.3)$$

where the second inequality applies Lemma 2 to the Lipschitz functions $\{g\}$.

Suppose the radius r satisfies

$$r^2 \geq 6M\mathbb{E}R_n\{f-f_* : f \in \mathcal{F}, \|f-f_*\|_{L_2(X)} \leq r\} \qquad (A.4)$$

and

$$r^2 \geq \frac{8M^2\gamma}{n}. \qquad (A.5)$$

Then we conclude from from (A.3) that

$$\mathbb{E}_n(f-f_*)^2 \leq r^2 + r^2 + 2Mr\sqrt{\frac{2\gamma}{n}} + \frac{16M^2}{3}\frac{\gamma}{n} \leq (2r)^2 \qquad (A.6)$$

where the first inequality uses (A.4) and the second line uses (A.5). This means that for r above the "critical radius" (see **Step III**), the empirical L_2-norm is at most twice the population one with probability at least $1 - \exp(-\gamma)$.

A.2.2 Step II: One Step Improvement

In this step we will show that given a bound on $\|\hat{f} - f_*\|_{L_2(X)}$ we can use this bound as information to obtain a tighter bound, if the initial bound is loose as made precise at the end of this step. Suppose we know that for some r_0, $\|\hat{f} - f_*\|_{L_2(X)} \leq r_0$ and, by **Step I**, $\|\hat{f} - f_*\|_n \leq 2r_0$. We may always start with $r_0 = 2M$ given Assumption 1 and (2.3). Apply Lemma 6 with $\mathcal{G} := \{g = \ell(f, \boldsymbol{z}) - \ell(f_*, \boldsymbol{z}) : f \in \mathcal{F}_{\text{DNN}}, \|f - f_*\|_{L_2(X)} \leq r_0\}$, we find that, with probability at least $1 - 2e^{-\gamma}$, the empirical process term of (A.1) is bounded as

$$(\mathbb{E} - \mathbb{E}_n)\left[\ell(\hat{f}, \boldsymbol{z}) - \ell(f_*, \boldsymbol{z})\right] \leq 6\mathbb{E}_\eta R_n \mathcal{G} + \sqrt{\frac{2C_\ell^2 r_0^2 \gamma}{n}} + \frac{46MC_\ell}{3}\frac{\gamma}{n}, \tag{A.7}$$

where the middle term is due to the following variance calculation (recall Lemma 10)

$$\mathbb{V}[g] \leq \mathbb{E}[g^2] = \mathbb{E}[|\ell(f, \boldsymbol{z}) - \ell(f_*, \boldsymbol{z})|^2] \leq C_\ell^2 \mathbb{E}(f - f_*)^2 \leq C_\ell^2 r_0^2$$

and the final term follows because the right side of (C.1) is bounded by $C_\ell 2M$. Here the fact that Lemma 6 is variance dependent, and that the variance depends on the radius r_0, is important. It is this property which enables a sharpening of the rate with step-by-step reductions in the variance bound, as in Section A.2.4.

For the empirical Rademacher complexity term, the first term of (A.7), Lemma 2, **Step I**, and Lemma 3, yield

$$\begin{aligned}
\mathbb{E}_\eta R_n \mathcal{G} &= \mathbb{E}_\eta R_n \{g : g = \ell(f, \boldsymbol{z}) - \ell(f_*, \boldsymbol{z}), f \in \mathcal{F}_{\text{DNN}}, \|f - f_*\| \leq r_0\} \\
&\leq C_\ell \mathbb{E}_\eta R_n \{f - f_* : f \in \mathcal{F}_{\text{DNN}}, \|f - f_*\| \leq r_0\} \\
&\leq C_\ell \mathbb{E}_\eta R_n \{f - f_* : f \in \mathcal{F}_{\text{DNN}}, \|f - f_*\|_n \leq 2r_0\} \\
&\leq C_\ell \inf_{0 < \alpha < 2r_0} \left\{ 4\alpha + \frac{12}{\sqrt{n}} \int_\alpha^{2r_0} \sqrt{\log \mathcal{N}(\delta, \mathcal{F}_{\text{DNN}}, \|\cdot\|_n)} d\delta \right\} \\
&\leq C_\ell \inf_{0 < \alpha < 2r_0} \left\{ 4\alpha + \frac{12}{\sqrt{n}} \int_\alpha^{2r_0} \sqrt{\log \mathcal{N}(\delta, \mathcal{F}_{\text{DNN}}|_{x_1,\ldots,x_n}, \infty)} d\delta \right\},
\end{aligned}$$

Recall Lemma 4, one can further upper bound the entropy integral when $n > \text{Pdim}(\mathcal{F}_{\text{DNN}})$,

$$\begin{aligned}
&\inf_{0 < \alpha < 2r_0} \left\{ 4\alpha + \frac{12}{\sqrt{n}} \int_\alpha^{2r_0} \sqrt{\log \mathcal{N}(\delta, \mathcal{F}_{\text{DNN}}|_{x_1,\ldots,x_n}, \infty)} d\delta \right\} \\
&\leq \inf_{0 < \alpha < 2r_0} \left\{ 4\alpha + \frac{12}{\sqrt{n}} \int_\alpha^{2r_0} \sqrt{\text{Pdim}(\mathcal{F}_{\text{DNN}}) \log \frac{2eMn}{\delta \cdot \text{Pdim}(\mathcal{F}_{\text{DNN}})}} d\delta \right\}
\end{aligned}$$

$$\leq 32 r_0 \sqrt{\frac{\mathrm{Pdim}(\mathcal{F}_{\mathrm{DNN}})}{n} \left(\log \frac{2eM}{r_0} + \frac{3}{2} \log n \right)}$$

with a particular choice of $\alpha = 2r_0 \sqrt{\mathrm{Pdim}(\mathcal{F}_{\mathrm{DNN}})/n} < 2r_0$. Therefore, whenever $r_0 \geq 1/n$ and $n \geq (2eM)^2$,

$$\mathbb{E}_\eta R_n \mathcal{G} \leq 64 C_\ell r_0 \sqrt{\frac{\mathrm{Pdim}(\mathcal{F}_{\mathrm{DNN}})}{n}} \log n.$$

Applying this bound to (A.7), we have

$$(\mathbb{E} - \mathbb{E}_n) \left[\ell(\hat{f}, \boldsymbol{z}) - \ell(f_*, \boldsymbol{z}) \right] \leq K r_0 \sqrt{\frac{\mathrm{Pdim}(\mathcal{F}_{\mathrm{DNN}})}{n}} \log n + r_0 \sqrt{\frac{2 C_\ell^2 \gamma}{n}} + \frac{46 M C_\ell}{3} \frac{\gamma}{n} \qquad \text{(A.8)}$$

where $K = 6 \times 64 C_\ell$.

Going back now to the main decomposition, plug (A.8) and (A.2) into (A.1), and we find that

$$
\begin{aligned}
& c_2 \| \hat{f} - f_* \|_{L_2(X)}^2 \\
& \leq K r_0 \sqrt{\frac{\mathrm{Pdim}(\mathcal{F}_{\mathrm{DNN}})}{n}} \log n + r_0 \sqrt{\frac{2 C_\ell^2 \gamma}{n}} + \frac{46 M C_\ell}{3} \frac{\gamma}{n} + \left(\frac{1}{c_2} \epsilon^2 + \epsilon \sqrt{\frac{2 C_\ell^2 \gamma}{n}} + \frac{14 C_\ell M \gamma}{3n} \right) \\
& \leq r_0 \cdot \left(K \sqrt{\frac{\mathrm{Pdim}(\mathcal{F}_{\mathrm{DNN}})}{n}} \log n + \sqrt{\frac{2 C_\ell^2 \gamma}{n}} \right) + \epsilon_n^2 + \epsilon_n \sqrt{\frac{2 C_\ell^2 \gamma}{n}} + 20 M C_\ell \frac{\gamma}{n} \\
& \leq r_0 \cdot \left(K \sqrt{C} \sqrt{\frac{W L \log W}{n}} \log n + \sqrt{\frac{2 C_\ell^2 \gamma}{n}} \right) + \epsilon_n^2 + \epsilon_n \sqrt{\frac{2 C_\ell^2 \gamma}{n}} + 20 M C_\ell \frac{\gamma}{n}, \qquad \text{(A.9)}
\end{aligned}
$$

with probability at least $1 - 3 \exp(-\gamma)$, where the last line applies Lemma 7. Therefore, whenever $\epsilon_n \ll r_0$ and $\sqrt{\frac{W L \log W}{n}} \log n \ll r_0$, the knowledge that $\| \hat{f} - f_* \|_{L_2(X)} \leq r_0$ implies that (with high probability) $\| \hat{f} - f_* \|_{L_2(X)} \leq r_1$, for $r_1 \ll r_0$. One can recursively improve the bound r to a fixed point/radius r_*, which describes the fundamental difficulty of the problem. This is done in the course of the next two steps.

A.2.3 Step III: Critical Radius

Formally, define the critical radius r_* to be the largest fixed point

$$r_* = \inf \left\{ r > 0 : 6 M \mathbb{E} R_n \{ f - f_* : f \in \mathcal{F}, \| f - f_* \|_{L_2(X)} \leq s \} < s^2, \forall u \geq r \right\}.$$

By construction this obeys (A.4), and thus so does $2r_*$. Denote the event E (depending on the data) to be

$$E = \left\{ \| f - f_* \|_n \leq 4 r_*, \text{ for all } f \in \mathcal{F} \text{ and } \| f - f_* \|_{L_2(X)} \leq 2 r_* \right\}$$

and $\mathbb{1}_E$ to be the indicator that event E holds. We know from (A.6) that $\mathbb{P}(\mathbb{1}_E = 1) \geq 1 - n^{-1}$, provided $r_* \geq \sqrt{8}M\sqrt{\log n/n}$ to satisfy (A.5).

We can now give an upper bound for the the critical radius r_*. Using the logic of **Step II** to bound the empirical Rademacher complexity, and then applying Lemma 7, we find that

$$
\begin{aligned}
r_*^2 &\leq 6M\mathbb{E}R_n\big\{f - f_* : f \in \mathcal{F}, \|f - f_*\|_{L_2(X)} \leq r_*\big\} \\
&\leq 6M\mathbb{E}R_n\big\{f - f_* : f \in \mathcal{F}, \|f - f_*\|_{L_2(X)} \leq 2r_*\big\} \\
&\leq 6M\mathbb{E}\big\{\mathbb{E}_\eta R_n\{f - f_* : f \in \mathcal{F}, \|f - f_*\|_n \leq 4r_*\}\mathbb{1}_E + 2M(1 - \mathbb{1}_E)\big\} \\
&\leq 12MK\sqrt{C} \cdot r_*\sqrt{\frac{WL\log W}{n}\log n} + 12M^2\frac{1}{n} \\
&\leq 14MK\sqrt{C} \cdot r_*\sqrt{\frac{WL\log W}{n}\log n},
\end{aligned}
$$

with the last line relying on the above restriction that $r_* \geq \sqrt{8}M\sqrt{\log n/n}$. Dividing through by r_* yields the final bound:

$$
r_* \leq 14MK\sqrt{C}\sqrt{\frac{WL\log W}{n}\log n}. \tag{A.10}
$$

A.2.4 Step III: Localization

Divide the space $\mathcal{F}_{\mathrm{DNN}}$ into shells of increasing radius by intersecting it with the balls

$$
B(f_*, \bar{r}), B(f_*, 2\bar{r})\backslash B(f_*, \bar{r}), \ldots B(f_*, 2^l\bar{r})\backslash B(f_*, 2^{l-1}\bar{r}) \tag{A.11}
$$

where $l \leq \log_2 \frac{2M}{\sqrt{(\log n)/n}}$. We will specify the choice of $\bar{r}$ shortly.

Suppose $\bar{r} > r_*$. Then for each shell, **Step I** implies that with probability at least $1 - 2l\exp(-\gamma)$,

$$
\|f - f_*\|_{L_2(X)} \leq 2^j\bar{r} \implies \|f - f_*\|_n \leq 2^{j+1}\bar{r}. \tag{A.12}
$$

Further, suppose that for some $j \leq l$

$$
\hat{f} \in B(f_*, 2^j\bar{r})\backslash B(f_*, 2^{j-1}\bar{r}). \tag{A.13}
$$

Then applying the one step improvement argument in **Step II** (again the variance dependence captured in Lemma 6 is crucial, here reflected in the variance within each shell), Equation (A.9) yields that with probability at least $1 - 3\exp(-\gamma)$,

$$
\begin{aligned}
\|\hat{f} - f_*\|_{L_2(X)}^2 &\leq \frac{1}{c_2}\left\{2^j\bar{r} \cdot \left(K\sqrt{C}\sqrt{\frac{WL\log W}{n}\log n} + \sqrt{\frac{2C_\ell^2 t}{n}}\right) + \epsilon_n^2 + \epsilon_n\sqrt{\frac{2C_\ell^2\gamma}{n}} + 20MC_\ell\frac{\gamma}{n}\right\} \\
&\leq 2^{2j-2}\bar{r}^2,
\end{aligned}
$$

47

if the following two conditions hold:

$$\frac{1}{c_2}\left(K\sqrt{C}\sqrt{\frac{WL\log W}{n}}\log n + \sqrt{\frac{2C_\ell^2\gamma}{n}}\right) \le \frac{1}{8}2^j\bar{r}$$

$$\frac{1}{c_2}\left(\epsilon_n^2 + \epsilon_n\sqrt{\frac{2C_\ell^2 t}{n}} + 26MC_\ell\frac{\gamma}{n}\right) \le \frac{1}{8}2^{2j}\bar{r}^2.$$

It is easy to see that these two hold for all j if we choose

$$\bar{r} = \frac{8}{c_2}\left(K\sqrt{C}\sqrt{\frac{WL\log W}{n}}\log n + \sqrt{\frac{2C_\ell^2\gamma}{n}}\right) + \left(\sqrt{\frac{16}{c_2}}\epsilon_n + \sqrt{\frac{208MC_\ell}{c_2}\frac{\gamma}{n}}\right) + r_*. \qquad (A.14)$$

Therefore with probability at least $1 - 5l\exp(-\gamma)$, we can perform shell-by-shell argument combining the results in **Step I** and **Step II**:

$$\|\hat{f} - f_*\|_{L_2(X)} \le 2^l\bar{r} \text{ and } \|\hat{f} - f_*\|_n \le 2^{l+1}\bar{r}$$
$$\text{implies } \|\hat{f} - f_*\|_{L_2(X)} \le 2^{l-1}\bar{r} \text{ and } \|\hat{f} - f_*\|_n \le 2^l\bar{r}$$
$$\cdots\cdots$$
$$\text{implies } \|\hat{f} - f_*\|_{L_2(X)} \le 2^0\bar{r} \text{ and } \|\hat{f} - f_*\|_n \le 2^1\bar{r}.$$

The "and" part of each line follows from **Step I** and the implication uses the above argument following **Step II**. Therefore in the end, we conclude with probability at least $1 - 5l\exp(-t)$,

$$\|\hat{f} - f_*\|_{L_2(X)} \le \bar{r} \ , \qquad (A.15)$$
$$\|\hat{f} - f_*\|_n \le 2\bar{r} \ . \qquad (A.16)$$

Therefore choose $\gamma = \log(5l) + \gamma'$, we know from (A.14), and the upper bound on r_* in (A.10)

$$\bar{r} \le \frac{8}{c_2}\left(K\sqrt{C}\sqrt{\frac{WL\log W}{n}}\log n + \sqrt{\frac{2C_\ell^2(\log\log n + \gamma')}{n}}\right) + \left(\sqrt{\frac{16}{c_2}}\epsilon_n + \sqrt{\frac{208MC_\ell}{c_2}\frac{\log\log n + \gamma'}{n}}\right) + r_*$$

$$\le C'\left(\sqrt{\frac{WL\log W}{n}}\log n + \sqrt{\frac{\log\log n + \gamma'}{n}} + \epsilon_n\right), \qquad (A.17)$$

with some absolute constant $C' > 0$. This completes the proof of Theorem 2.

A.3 Final Steps for the MLP case

For the multi-layer perceptron, $W \leq C \cdot H^2 L$, and plugging this into the bound (A.17), we obtain

$$C' \left(\sqrt{\frac{H_n^2 L_n^2 \log(H_n^2 L_n)}{n}} \log n + \sqrt{\frac{\log \log n + t'}{n}} + \epsilon_n \right)$$

To optimize this upper bound on $\bar{r}$, we need to specify the trade-offs in ϵ_n and H_n and L_n. To do so, we utilize the MLP-specific approximation rate of Lemma 8 and the embedding of Lemma 1. Lemma 1 implies that, for any ϵ_n, one can embed the approximation class $\mathcal{F}_{\text{DNN}}$ given by Lemma 8 into a standard MLP architecture $\mathcal{F}_{\text{MLP}}$, where specifically

$$H_n = H(\epsilon_n) \leq W(\epsilon_n)L(\epsilon_n) \leq C^2 \epsilon_n^{-\frac{d}{\beta}} (\log(1/\epsilon_n) + 1)^2,$$
$$L_n = L(\epsilon_n) \leq C \cdot (\log(1/\epsilon_n) + 1).$$

For standard MLP architecture $\mathcal{F}_{\text{MLP}}$,

$$H_n^2 L_n^2 \log(H_n^2 L_n) \leq \tilde{C} \cdot \epsilon_n^{-\frac{2d}{\beta}} (\log(1/\epsilon_n) + 1)^7.$$

Thus we can optimize the upper bound

$$\bar{r} \leq C' \left(\sqrt{\frac{\epsilon_n^{-\frac{2d}{\beta}} (\log(1/\epsilon_n) + 1)^7}{n}} \log n + \sqrt{\frac{\log \log n + \gamma'}{n}} + \epsilon_n \right)$$

by choosing $\epsilon_n = n^{-\frac{\beta}{2(\beta+d)}}$, $H_n = c_1 \cdot n^{\frac{d}{2(\beta+d)}} \log^2 n$, $L_n = c_2 \cdot \log n$. This gives

$$\bar{r} \leq C \left(n^{-\frac{\beta}{2(\beta+d)}} \log^4 n + \sqrt{\frac{\log \log n + t'}{n}} \right).$$

Hence putting everything together, with probability at least $1 - \exp(-\gamma)$,

$$\mathbb{E}(\hat{f} - f_*)^2 \leq \bar{r}^2 \leq C \left(n^{-\frac{\beta}{\beta+d}} \log^8 n + \frac{\log \log n + \gamma}{n} \right),$$
$$\mathbb{E}_n(\hat{f} - f_*)^2 \leq (2\bar{r})^2 \leq 4C \left(n^{-\frac{\beta}{\beta+d}} \log^8 n + \frac{\log \log n + \gamma}{n} \right).$$

This completes the proof of Theorem 1.

B   Proof of Corollaries 1 and 2

For Corollary 1, we want to optimize

$$\frac{WL \log U}{n} \log n + \frac{\log \log n + \gamma}{n} + \epsilon_{\text{DNN}}^2.$$

Yarotsky (2017, Theorem 1) shows that for the approximation error ϵ_{DNN} to obey $\epsilon_{\text{DNN}} \leq \epsilon$, it suffices to choose $W, U \propto \epsilon^{-\frac{d}{\beta}}(\log(1/\epsilon) + 1)$ and $L \propto (\log(1/\epsilon) + 1)$, given the specific architecture described therein. Therefore, we attain $\epsilon \asymp n^{-\beta/(2\beta+d)}$ by setting $W, U \asymp n^{d/(2\beta+d)}$ and $L \asymp \log n$, yielding the desired result.

For Corollary 2, we need to optimize

$$\frac{H^2 L_2 \log(HL)}{n} \log n + \frac{\log \log n + \gamma}{n} + \epsilon_{\text{MLP}}^2.$$

Yarotsky (2018, Theorem 1) shows that for the approximation error ϵ_{MLP} to obey $\epsilon_{\text{MLP}} \leq \epsilon$, it suffices to choose $H \propto 2d + 10$ and $L \propto \epsilon^{-\frac{d}{2}}$, given the specific architecture described therein. Thus, for $\epsilon \asymp n^{-1/(2+d)}$ we take $L \asymp n^{-d/(4+2d)}$, and the result follows.

C   Supporting Lemmas

First, we show that one can embed a feedforward network into the multi-layer perceptron architecture by adding auxiliary hidden nodes. This idea is due to Yarotsky (2018).

Lemma 1 (Embedding). *For any function $f \in \mathcal{F}_{\text{DNN}}$, there is a $g \in \mathcal{F}_{\text{MLP}}$, with $H \leq WL + U$, such that $g = f$.*
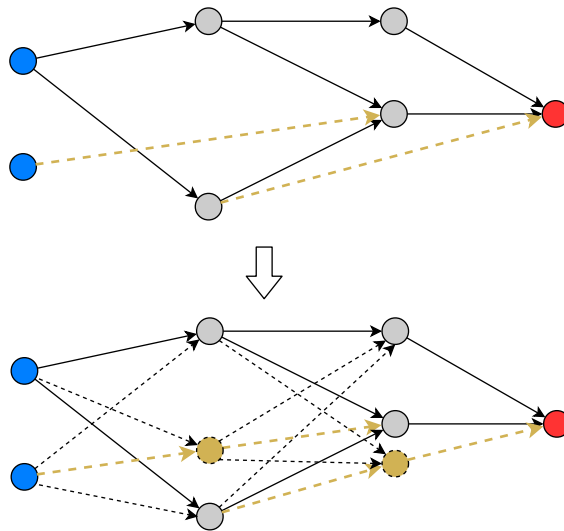

Figure 6: Illustration of how to embed a feedforward network into a multi-layer perceptron, with auxiliary hidden nodes (shown in yellow).

Proof. The idea is illustrated in Figure 6. For the edges in the directed graph of $f \in \mathcal{F}_{\mathrm{DNN}}$ that connect nodes not in adjacent layers (shown in yellow in Figure 6), one can insert auxiliary hidden units in order to simply "pass forward" the information. The number of such auxiliary "passforward units" is at most the number of offending edges times the depth L (i.e. for each edge, at most L auxiliary nodes are required), and this is bounded by WL. Therefore the width of the MLP network that subsumes the original is upper bounded by $WL + U$ while still maintaining the required embedding that for any $f_\theta \in \mathcal{F}_{\mathrm{DNN}}$, there is a $g_{\theta'} \in \mathcal{F}_{\mathrm{MLP}}$ such that $g_{\theta'} = f_\theta$. In order to match modern practice we only need to show that auxiliary units can be implemented with ReLU activation. This can be done by setting the constant ("bias") term b of each auxiliary unit large enough to ensure $\sigma(\tilde{\boldsymbol{x}}'\boldsymbol{w} + b) = \tilde{\boldsymbol{x}}'\boldsymbol{w} + b$, and then subtracting the same b in the last receiving unit along the path. $\qquad\square$

Next, we give two properties of the Rademacher complexity that we require (see Mendelson, 2003).

Lemma 2 (Contraction). *Let $\phi : \mathbb{R} \to \mathbb{R}$ be a Lipschitz contraction $|\phi(x) - \phi(y)| \leq L|x - y|$, then*

$$\mathbb{E}_\eta R_n\{\phi \circ f : f \in \mathcal{F}\} \leq L\mathbb{E}_\eta R_n \mathcal{F}.$$

Lemma 3 (Dudley's Chaining). *Let $\mathcal{N}(\delta, \mathcal{F}, \|\cdot\|_n)$ denote the metric entropy for class $\mathcal{F}$ (with covering radius δ and metric $\|\cdot\|_n$), then*

$$\mathbb{E}_\eta R_n\{f : f \in \mathcal{F}, \|f\|_n \leq r\} \leq \inf_{0 < \alpha < r} \left\{ 4\alpha + \frac{12}{\sqrt{n}} \int_\alpha^r \sqrt{\log \mathcal{N}(\delta, \mathcal{F}, \|\cdot\|_n)} d\delta \right\} .$$

Furthermore, because $\|f\|_n \leq \max_i |f(\boldsymbol{x}_i)|$, and therefore $\mathcal{N}(\delta, \mathcal{F}, \|\cdot\|_n) \leq \mathcal{N}(\delta, \mathcal{F}|_{\boldsymbol{x}_1,\ldots,\boldsymbol{x}_n}, \infty)$ and so the upper bound in the conclusions also holds with $\mathcal{N}(\delta, \mathcal{F}|_{\boldsymbol{x}_1,\ldots,\boldsymbol{x}_n}, \infty)$.

The next two results, Theorems 12.2 and 14.1 in Anthony and Bartlett (1999), show that the metric entropy may be bounded in terms of the pseudo-dimension and that the latter is bounded by the Vapnik-Chervonenkis (VC) dimension.

Lemma 4. *Assume for all $f \in \mathcal{F}$, $\|f\|_\infty \leq M$. Denote the pseudo-dimension of $\mathcal{F}$ as $\mathrm{Pdim}(\mathcal{F})$, then for $n \geq \mathrm{Pdim}(\mathcal{F})$, we have for any δ,*

$$\mathcal{N}(\delta, \mathcal{F}|_{x_1,\ldots,x_n}, \infty) \leq \left(\frac{2eM \cdot n}{\delta \cdot \mathrm{Pdim}(\mathcal{F})} \right)^{\mathrm{Pdim}(\mathcal{F})} .$$

Lemma 5. *If $\mathcal{F}$ is the class of functions generated by a neural network with a fixed architecture and fixed activation functions, then*

$$\mathrm{Pdim}(\mathcal{F}) \leq \mathrm{VCdim}(\tilde{\mathcal{F}})$$

where $\tilde{\mathcal{F}}$ has only one extra input unit and one extra computation unit compared to $\mathcal{F}$.

The following symmetrization lemma bounds the empirical processes term using Rademacher complexity, and is thus a crucial piece of our localization. This is a standard result based on Talagrand's concentration, but here special care is taken with the dependence on the variance.

Lemma 6 (Symmetrization, Theorem 2.1 in Bartlett, Bousquet, Mendelson, et al. (2005))**.** *For any $g \in \mathcal{G}$, assume that $|g| \leq G$ and $\mathbb{V}[g] \leq V$. Then for every $\gamma > 0$, with probability at least $1 - e^{-\gamma}$*

$$\sup_{g \in \mathcal{G}} \{\mathbb{E}g - \mathbb{E}_n g\} \leq 3\mathbb{E}R_n \mathcal{G} + \sqrt{\frac{2V\gamma}{n}} + \frac{4G}{3}\frac{\gamma}{n} \ ,$$

and with probability at least $1 - 2e^{-t}$

$$\sup_{g \in \mathcal{G}} \{\mathbb{E}g - \mathbb{E}_n g\} \leq 6\mathbb{E}_\eta R_n \mathcal{G} + \sqrt{\frac{2V\gamma}{n}} + \frac{23G}{3}\frac{\gamma}{n} \ .$$

The same result holds for $\sup_{g \in \mathcal{G}} \{\mathbb{E}_n g - \mathbb{E}g\}$.

In turn, when bounding the complexity using the VC dimension of $\mathcal{F}_{\mathrm{DNN}}$, we use the following bounds on the latter.

Lemma 7 (Theorem 6 in Bartlett, Harvey, Liaw, and Mehrabian (2017), ReLU case)**.** *Consider a ReLU network architecture $\mathcal{F} = \mathcal{F}_{\mathrm{DNN}}(W, L, U)$, then the VC-dimension and pseudo-dimension is sandwiched by*

$$c \cdot WL \log(W/L) \leq \mathrm{VCdim}(\mathcal{F}) \leq C \cdot WL \log W,$$

with some universal constants $c, C > 0$. The same result holds for $\mathrm{Pdim}(\mathcal{F})$.

For multi-layer perceptrons we use the following approximation result, Theorem 1 of Yarotsky (2017).

Lemma 8. *There exists a network class $\mathcal{F}_{\mathrm{DNN}}$, with ReLU activation, such that for any $\epsilon > 0$:*

(a) *$\mathcal{F}_{\mathrm{DNN}}$ approximates the $W^{\beta,\infty}([-1,1]^d)$ in the sense for any $f_* \in W^{\beta,\infty}([-1,1]^d)$, there exists a $f_n(\epsilon) := f_n \in \mathcal{F}_{\mathrm{DNN}}$ such that*

$$\|f_n - f_*\|_\infty \leq \epsilon,$$

(b) *and $\mathcal{F}_{\mathrm{DNN}}$ has $L(\epsilon) \leq C \cdot (\log(1/\epsilon) + 1)$ and $W(\epsilon), U(\epsilon) \leq C \cdot \epsilon^{-\frac{d}{\beta}}(\log(1/\epsilon) + 1)$.*

Here C only depends on d and β.

The next two lemmas relate differences in the loss to differences in the functions themselves. These are used at very steps and follow from standard calculus arguments.

Lemma 9 (Curvature)**.** *For Both the least squares (2.1) and logistic (2.2) loss functions*

$$c_1\mathbb{E}\left[(f - f_*)^2\right] \leq \mathbb{E}[\ell(f, \mathbf{Z})] - \mathbb{E}\ell[(f_*, \mathbf{Z})] \leq c_2\mathbb{E}\left[(f - f_*)^2\right].$$

For least squares, $c_1 = c_2 = 1/2$. For logistic, $c_1 = (2(\exp(M) + \exp(-M) + 2))^{-1}$, $c_2 = 1/8$.

Proof. For least squares, using iterated expectations

$$2\mathbb{E}\ell(f, \boldsymbol{Z}) - 2\mathbb{E}\ell(f_*, \boldsymbol{Z}) = \mathbb{E}\left[-2Yf + f^2 + 2Yf_* - f_*^2\right]$$
$$= \mathbb{E}\left[-2f_*f(\boldsymbol{x}) + f^2 + 2(f_*)^2 - f_*^2\right]$$
$$= \mathbb{E}\left[(f - f_*)^2\right].$$

For logistic regression,

$$\mathbb{E}[\ell(f, \boldsymbol{Z})] - \mathbb{E}[\ell(f_*, \boldsymbol{Z})] = \mathbb{E}\left[-\frac{\exp(f_*)}{1 + \exp(f_*)}(f - f_*) + \log\left(\frac{1 + \exp(f)}{1 + \exp(f_*)}\right)\right].$$

Define $h_a(b) = -\frac{\exp(a)}{1+\exp(a)}(b - a) + \log\left(\frac{1+\exp(b)}{1+\exp(a)}\right)$, then

$$h_a(b) = h_a(a) + h_a'(a)(b - a) + \frac{1}{2}h_a''\left(\xi a + (1 - \xi)b\right)(b - a)^2$$

and $h_a''(b) = \frac{1}{\exp(b)+\exp(-b)+2} \leq \frac{1}{4}$. The lower bound holds as $|\xi f_* + (1 - \xi)f| \leq M$. $\qquad\square$

Lemma 10 (Lipschitz)**.** *For Both the least squares* (2.1) *and logistic* (2.2) *loss functions*

$$|\ell(f, \boldsymbol{z}) - \ell(g, \boldsymbol{z})| \leq C_\ell|f(\boldsymbol{x}) - g(\boldsymbol{x})|. \tag{C.1}$$

For least squares, $C_\ell = M$. For logistic regression, $C_\ell = 1$.

Our last result is to verify condition (c) of Theorem 3. We do so using our localization, which may be of future interest in second-step inference with machine learning methods.

Lemma 11. *Let the conditions of Theorem 3 hold. Then*

$$\mathbb{E}_n\left[(\hat{\mu}_t(\boldsymbol{x}_i) - \mu_t(\boldsymbol{x}_i))\left(1 - \frac{\mathbb{1}\{t_i = t\}}{\mathbb{P}[T = t|\boldsymbol{X} = \boldsymbol{x}_i]}\right)\right] = o_P\left(n^{-\frac{\beta}{\beta+d}}\log^8 n + \frac{\log\log n}{n}\right) = o_P\left(n^{-1/2}\right).$$

Proof. Without loss of generality we can take $\bar{p} < 1/2$. The only estimated function here is $\mu_t(\boldsymbol{x})$, which plays the role of f_* here. For function(als) $L(\cdot)$ of the form

$$L(f) := (f(\boldsymbol{x}_i) - f_*(\boldsymbol{x}_i))\left(1 - \frac{\mathbb{1}\{t_i = t\}}{\mathbb{P}[T = t|\boldsymbol{X} = \boldsymbol{x}_i]}\right),$$

it is true that

$$\mathbb{E}[L(f)] = \mathbb{E}\left[(f(\boldsymbol{X}) - f_*(\boldsymbol{X}))\left(1 - \frac{\mathbb{E}[\mathbb{1}\{t_i = t\}|\boldsymbol{x}_i]}{\mathbb{P}[T = t|\boldsymbol{X} = \boldsymbol{x}_i]}\right)\right] = 0$$

and

$$\mathbb{V}[L(f)] \leq (1/\bar{p} - 1)^2 \, \mathbb{E}\left[(f(\boldsymbol{X}) - f_*(\boldsymbol{X}))^2\right] \leq (1/\bar{p} - 1)^2 \, \bar{r}^2$$
$$|L(f)| \leq (1/\bar{p} - 1)\, 2M.$$

For $\bar{r}$ defined in (A.14),

$$6M\mathbb{E}R_n\{f - f_* : f \in \mathcal{F}, \|f - f_*\|_{L_2(X)} \leq \bar{r}\} \leq \bar{r}^2$$
$$\mathbb{E}R_n\{L(f) : f \in \mathcal{F}, \|f - f_*\|_{L_2(X)} \leq \bar{r}\} \leq (1/\bar{p} - 1)\, \mathbb{E}R_n\{f - f_* : f \in \mathcal{F}, \|f - f_*\|_{L_2(X)} \leq \bar{r}\}$$

where the first line is due to $\bar{r} > r_*$, and second line uses Lemma 2.

Then by the localization analysis and Lemma 6, for all $f \in \mathcal{F}, \|f - f_*\|_{L_2(X)} \leq \bar{r}$, $L(f)$ obeys

$$\mathbb{E}_n[L(f)] = \mathbb{E}_n[L(f)] - \mathbb{E}[L(f)] \leq 3C\bar{r}^2 + \bar{r}\sqrt{\frac{2\,(1/\bar{p} - 1)^2\, t}{n}} + \frac{4\,(1/\bar{p} - 1)\, 2M}{3}\frac{t}{n} \leq 4C\bar{r}^2$$
$$\leq C \cdot \left\{ n^{-\frac{\beta}{\beta + d}} \log^8 n + \frac{\log \log n}{n} \right\},$$
$$\sup_{f \in \mathcal{F}, \|f - f_*\|_{L_2(X)} \leq \bar{r}} \mathbb{E}_n[L(f)] \leq C \cdot \left\{ n^{-\frac{\beta}{\beta + d}} \log^8 n + \frac{\log \log n}{n} \right\}.$$

With probability at least $1 - \exp(-n^{\frac{d}{\beta + d}} \log^8 n)$, $\hat{f}_{\mathrm{MLP}}$ lies in this set of functions, and therefore

$$\mathbb{E}_n[L(\hat{f}_{\mathrm{MLP}})] = \mathbb{E}_n\left[(\widehat{f}_{n,H,L}(x) - f_*(x))\left(1 - \frac{1(T = t)}{P(T = t|\boldsymbol{x} = x)}\right)\right] \leq C \cdot \left\{ n^{-\frac{\beta}{\beta + d}} \log^8 n + \frac{\log \log n}{n} \right\},$$

as claimed. $\qquad\square$